

# Numerical methods and analytic results for one-dimensional strongly interacting spinor gases

Ovidiu I. Pătu<sup>1</sup>

<sup>1</sup>*Institute for Space Sciences, Bucharest-Măgurele, R 077125, Romania*

One of quantum physics' fundamental, but largely unsolved, problems is the computation of the correlation functions in many-body systems. In this paper we address this problem in the case of one-dimensional spinor gases with repulsive contact interactions in the presence of a confining potential. We take advantage of the fact that in the strong coupling limit, the wavefunction factorizes with the charge degrees of freedom expressed as a Slater determinant of spinless fermions and the spin sector described by a spin chain of Sutherland type with exchange coefficients that depend only on the trapping potential. This factorization is also present in the expressions for the correlation functions. Still, analytical and numerical investigations were hindered by the fact that the local exchange coefficients and the charge component of the correlators are expressed as  $N - 1$  multidimensional integrals, with  $N$  the number of particles, which are notoriously hard to compute using conventional methods. We introduce a new approach to calculating these integrals that is extremely simple, scales polynomially with the number of particles, and is several orders of magnitude faster than the previous methods reported in the literature. This allows us to investigate the static and dynamic properties, temperature dependence, and nonequilibrium dynamics for systems with a larger number of particles than previously considered and discover new phenomena. We show that, contrary to natural expectations, the momentum distribution of strongly interacting trapped spinor gases becomes narrower as we increase the temperature and derive simple determinant representations for the correlators in the spin incoherent regime valid for both equilibrium and nonequilibrium situations. For homogeneous systems of impenetrable particles at zero temperature we analytically compute the large distance asymptotics of the correlators finding that the leading term of the asymptotic expansion is proportional to  $e^{-x k_F \ln \kappa / \pi}$ , with  $\kappa$  the number of components of the system, which precludes any singularity of the momentum distribution.

## I. INTRODUCTION

One-dimensional (1D) quantum systems have received considerable interest in the last decades from both theoretical and experimental communities [1–3]. From the theoretical point of view this interest stems from the observation that quantum effects are enhanced in low dimensions coupled with the fact that many 1D quantum systems are integrable opening the way for comprehensive analytical and numerical investigations of the correlation functions and other physical quantities of interest [4, 5]. On the experimental side the unprecedented degree of control achieved in the manipulation of ultracold atomic gases resulted in the experimental realization of many paradigmatic 1D models [6–8] followed by subsequent investigations of many new intriguing phenomena specific to low-dimensional systems.

1D multicomponent systems are of particular importance because they present phases not found in their higher-dimensional counterparts and exhibit exotic phenomena like spin-charge separation [9]. In addition, their dynamics is expected to be very rich as a result of the interplay between the internal degrees of freedom, interaction, external fields and statistics of their constituents. In this paper we will consider spinor gases, bosonic or fermionic, with repulsive contact interactions subjected to a confining potential. These systems, also known as  $SU(\kappa)$  gases, with  $\kappa$  the number of components (internal degrees of freedom), are routinely realized in laboratories in both the few-body [10] and many-body [8] limits. In

the homogeneous case (no trapping potential) the spinor gases are integrable and in particular cases they reduce to some of the most well known models of 1D physics: the Lieb-Liniger model [11] for  $\kappa = 1$ , the Gaudin-Yang model [12, 13] for  $\kappa = 2$ , and the Sutherland models [14] for  $\kappa \geq 3$ . Fermionic systems have an antiferromagnetic ground state in accordance to Lieb-Mattis theorem [15] and at zero and low temperatures their correlation functions are described by bosonization and Luttinger liquid (LL) theory [9, 16]. While Lieb-Liniger (spinless) bosons are described at low temperatures by LL theory multicomponent bosons with spin independent interactions have a polarized ground state [17]. In this case the softest excitation above the ground state is the magnon mode with a quadratic dispersion relation which rules out the application of LL theory. This phase is a new low energy universality class called ferromagnetic liquid [18–21] with very distinct properties which are neither those of a localized ferromagnet nor of a Luttinger liquid. In the case of strong interactions the energy of the spin sector becomes much smaller than the energy of the charge sector  $E_{spin} \ll E_{charge}$ . When the thermal energy is much larger than the energy scale of the spin excitations but much smaller than the energy of the charge sector,  $E_{spin} \ll k_B T \ll E_{charge}$ , the fermionic and bosonic systems with  $\kappa \geq 2$  are described by the spin incoherent Luttinger liquid universality class (SILL) [22–28] which has a higher degree of universality than the LL and distinct properties.

In the strong coupling limit the Bethe ansatz wave-

functions of a homogeneous system factorize in spin and charge components with the charge degrees of freedom described by Slater determinants of free fermions and the spin sector characterized by a Sutherland type spin chain. This factorization was first noticed by Ogata and Shiba [29] in their investigation of the Hubbard model and represented the starting point of Izergin and Pronko's derivation of determinant representations for the correlators of the Gaudin-Yang model [30] in the SILL regime. Usually experiments are performed in the presence of a confining potential which breaks integrability. From general considerations it can be argued that the high degeneracy of the groundstate and the factorization of the wavefunctions remain valid for inhomogeneous systems with the charge degrees of freedom now being described by Slater determinants of spinless fermions subjected to the same trapping [31, 32]. In the case of the spin sector it took some time until it was realized that the Sutherland like spin chain that characterizes the spin degrees of freedom should have position variable coefficients which reflect the inhomogeneity of the trapping potential [33–39].

There are several advantages to this factorized description of strongly interacting spinor gases. The effective spin chain provides insights into the magnetic properties of spinor gases and the reduction of the Hilbert space allows for the investigation of larger number of particles than the conventional diagonalization methods employed for continuum systems. The spin sector can be studied using exact diagonalization for lattice systems or the Density Matrix Renormalization Group while the charge sector being described by spinless fermions in principle should be efficiently computed. In addition, one can also investigate more efficiently the low temperature correlators and the nonequilibrium dynamics. There are, however, some caveats. Knowledge of the wavefunction, while important, does not mean that the relevant physical quantities like the densities or momentum distributions are easily accessible. After all, we have known the wavefunctions of integrable systems like the Lieb-Liniger [11] and Gaudin-Yang [12, 13] models for almost 60 years and our understanding of their correlation functions is rather incomplete even in the case of single component systems while it is almost nonexistent for multicomponent models. The important feature is that the factorized nature of the wavefunction translates into the expressions for the correlation functions and one can compute the spin and charge components independently. One would expect that the computation of the spin functions would represent the limiting factor in the number of particles that can be investigated but this is not true. While the calculation of the spin sector properties is difficult at the present time the main computational bottleneck is represented by the calculation of the charge functions. The reason is that the position dependent coefficients appearing in the description of the effective spin chain, also known as local exchange coefficients, and the charge components of the correlators are expressed in terms of  $N - 1$

multidimensional integrals over products of Slater determinants, with  $N$  the number of particles, which are very hard to compute. Initial approaches used brute force or Monte-Carlo integration for systems up to 16 particles [33–41] followed by the introduction of more sophisticated methods which allowed for the computation of the coefficients for systems up to  $N = 35$  [42, 43] and  $N = 60$  [44] particles. The main drawbacks of these methods are the need for arbitrary precision calculations and the fact that they are very time consuming. For example, the calculation of the coefficients for  $N = 30$  takes about an hour [43, 44] and more than a week for  $N = 60$  [44]. These shortcomings are exacerbated in the case of nonequilibrium dynamics which requires the calculation of the local exchange coefficients at every step of the iterative process required to solve for the dynamics [45, 46]. The calculation of the charge functions for the correlators, also known as the one-body density matrix elements, is even more involved than the case of the local exchange coefficients with results for up to 20 particles being reported in [44]. An elegant method of computing the one-body density matrix elements using the connection with the correlation functions of 1D impenetrable anyons in the same geometry was introduced by Yang and Pu in [47] allowing for the investigation of harmonically trapped systems with up to 60 particles (see also [48]).

One of the main results of this paper is the introduction of an extremely efficient numerical method of calculating all the relevant charge functions: local exchange coefficients, single particle densities and one-body density matrix elements for any confining potential. Our method has a polynomial complexity in the number of particles, significantly outperforms all the other previously known algorithms, and is extremely simple requiring only the calculation of determinants involving partial overlaps of the single particle basis and the Discrete Fourier Transform. It is also exact with the only source of errors being the accuracy with which the partial overlaps of the single particle orbitals can be computed and does not require the use of arbitrary precision subroutines. For example, we are able to compute the local exchange coefficients in the case of harmonic trapping in less than 2 seconds for  $N = 60$  and in less than 30 seconds for  $N = 120$ . The one-body density matrix elements for 20 particles are computed in 0.015 seconds (compared with 742 seconds using the code provided in the ancillary files of [44]) and in less than a second for  $N = 60$ . We use this method to determine the density profiles and momentum distributions for harmonically trapped two-component fermionic and bosonic gases with  $N = 26$  particles for different values of the spin imbalance. We extract the Tan contacts of each component from the  $C_\sigma/k^4$  tails of the momentum distributions (the spectrum of the effective spin chain can be used to compute only the total contact) and show that for fermionic gases the contacts decrease as a function of the spin imbalance with the maximum obtained for the balanced system while in the case of bosonic gases the

total contact is constant with each individual contact increasing or decreasing linearly as a function of imbalance.

An important and interesting feature of strongly interacting spinor gases in 1D is that small changes in temperature can produce dramatic changes in the momentum distributions, spectral functions and transport properties of such systems [28]. We show that the transition from the LL/ferromagnetic liquid regime to the SILL phase is marked by a significant reconstruction of the momentum distribution in which the number of particles at large values of momenta decreases as the temperature is increased. This counterintuitive behavior, was probed indirectly in the case of two-component systems [49–51] but here we map the entire transition for two-, three-, and four-component systems and prove that is a general feature of multicomponent systems. The amplitude of this reconstruction is expected to decrease with the number of components. The way temperature influences the transport properties is investigated by studying the nonequilibrium dynamics after a quench from a domain wall boundary state [52]. At zero temperature, after the quench, the integrated magnetization as a function of time exhibits superdiffusive behaviour. At very small temperatures, for which the charge degrees of freedom are still close to the groundstate but the spin sector becomes incoherent, the integrated magnetization after the quench shows ballistic behaviour. This highlights the oversized role of the temperature in influencing the transport properties of strongly interacting spinor gases.

The main idea of our, mainly numerical, method can also be used to derive very efficient determinant representations for the space-, magnetic field-, and temperature-dependent correlators of impenetrable particles in the SILL regime. These representations are valid in both equilibrium and nonequilibrium situations generalizing the results of Pezer and Buljan [53] at zero temperature and Atas *et al.*, [54] at finite temperature for the single component bosonic Tonks-Girardeau gas. In the case of homogeneous systems at zero temperature we provide a Fredholm determinant representation in terms of the sine-kernel which contains as particular cases the well known results for single component bosons [55, 56] and two-component fermions and bosons [30]. We calculate analytically the large distance asymptotics of these correlators from the solution of the associated Riemann-Hilbert problem. The leading term of the asymptotics is given by  $e^{-xk_F \ln \kappa/\pi}$  implying that the momentum distributions of systems in the SILL regime do not present singularities even at zero temperature.

The plan of the paper is as follows. In Sec. II we review the 1D spinor gas and its eigenstates in the strongly interacting regime. In Sec. III we introduce the new method of computing the relevant charge quantities and in Sec. IV we present numerical results obtained using this new method. The determinant representations for the trapped and homogeneous systems in the SILL regime are derived in Sec. V and Sec. VI, respectively. We conclude in Sec. VII. Several technical details are rel-

egated to four appendices.

## II. ONE-DIMENSIONAL SPINOR GASES

We are interested in studying the static and dynamic properties of one-dimensional spinor gases with  $\kappa$  components and strong repulsive contact interactions. In the presence of an external confining potential  $V(z)$  the Hamiltonian in second quantization is

$$H = \int dz \frac{\hbar^2}{2m} (\partial_z \Psi^\dagger \partial_z \Psi) + \frac{g}{2} : (\Psi^\dagger \Psi)^2 : + V(z) (\Psi^\dagger \Psi) - \Psi^\dagger \mu \Psi, \quad (1)$$

where  $m$  is the mass of the particles,  $\Psi = (\Psi_1(z), \dots, \Psi_\kappa(z))^T$ ,  $\Psi^\dagger = (\Psi_1^\dagger(z), \dots, \Psi_\kappa^\dagger(z))$ ,  $:$  represents normal ordering,  $g > 0$  is the strength of the repulsive contact interaction and  $\mu$  is a matrix which has the chemical potentials  $\mu_1, \dots, \mu_\kappa$  of each component on the diagonal and zero otherwise. We consider fermionic or bosonic gases with the field operators in (1) satisfying the commutation relations

$$\Psi_\sigma(x) \Psi_{\sigma'}^\dagger(y) - \epsilon \Psi_{\sigma'}^\dagger(y) \Psi_\sigma(x) = \delta_{\sigma, \sigma'} \delta(x - y), \quad (2a)$$

$$\Psi_\sigma^\dagger(x) \Psi_{\sigma'}^\dagger(y) - \epsilon \Psi_{\sigma'}^\dagger(y) \Psi_\sigma^\dagger(x) = 0, \quad (2b)$$

$$\Psi_\sigma(x) \Psi_{\sigma'}(y) - \epsilon \Psi_{\sigma'}(y) \Psi_\sigma(x) = 0, \quad (2c)$$

where  $\sigma, \sigma' \in \{1, \dots, \kappa\}$  and  $\epsilon = 1 (-1)$  in the bosonic (fermionic) case. We will mainly use as an example the case of harmonic confinement  $V(z) = m\omega^2 z^2/2$  with  $\omega$  the trapping frequency but almost all the results derived in the paper remain true for any well behaved trapping potential including the case of Dirichlet boundary conditions in a system of dimension  $L$  which can be implemented by  $V(z) = 0$  for  $z \in [-L/2, L/2]$  and  $V(z) = \infty$  for  $z \notin [-L/2, L/2]$ . When the trapping potential is absent the Hamiltonian (1) is integrable for any value of the interaction strength and the wavefunctions and energy spectrum were obtained by Lieb and Liniger in [11] for the single component case, by Gaudin and Yang [12, 13] for  $\kappa = 2$  and in the general case by Sutherland in [14]. When an external potential is present the system is solvable only for  $g = 0$  and  $g = \infty$ .

In some applications it will also be useful to add to the Hamiltonian (1) a spin dependent magnetic gradient term of the form  $-Gz \Psi^\dagger \sigma^z \Psi$  [33, 37, 38] where  $\sigma^z$  is a generalized Pauli matrix with elements  $[\sigma^z]_{a,b} = \hbar(\frac{\kappa-1}{2} + 1 - b)\delta_{a,b}$  and  $G$  quantifies the strength of the gradient. In first quantization the Hamiltonian of the spinor gas with the magnetic gradient term is

$$\mathcal{H} = \left[ \sum_{j=1}^N -\frac{\hbar^2}{2m} \frac{\partial^2}{\partial z_j^2} + V(z_j) - Gz_j \sigma_j^z \right] + g \sum_{i < j} \delta(z_i - z_j) - \sum_{\sigma=1}^{\kappa} \mu_\sigma N_\sigma, \quad (3)$$

where  $N$  is the total number of particles and  $N_\sigma$  is the number of particles of type  $\sigma$ . From now on we will consider  $\hbar = m = \omega = 1$ .

### A. Groundstate manifold of eigenstates in the strongly interacting regime

A general eigenstate of the Hamiltonian (1) is given by

$$|\Phi\rangle = \int dz_1 \cdots dz_N \sum_{\substack{[N_1, \dots, N_\kappa] \\ \sigma_1, \dots, \sigma_N = \{1, \dots, \kappa\}}} \psi^{\sigma_1 \cdots \sigma_N}(z_1, \dots, z_N) \times \Psi_{\sigma_N}^\dagger(z_N) \cdots \Psi_{\sigma_1}^\dagger(z_1) |0\rangle, \quad (4)$$

with  $|0\rangle$  the Fock vacuum satisfying  $\Psi_\sigma(z)|0\rangle = 0$  for all values of  $\sigma$  and  $z$ . We will call such a state to be in the  $\mathbf{N}$  sector where we have introduced the notation  $\mathbf{N} = [N_1, \dots, N_\kappa]$  with  $\sum_{\sigma=1}^\kappa N_\sigma = N$ . In Eq. (4) the  $[N_1, \dots, N_\kappa]$  over the sum sign means that the sum is restricted such that the number of creation operators of type  $\sigma$  is  $N_\sigma$ . For arbitrary repulsion an explicit expression for the wavefunction  $\psi^{\sigma_1 \cdots \sigma_N}(z_1, \dots, z_N)$  is outside the reach of analytical methods but in the strongly interacting regime described by  $g$  very large but finite, the charge and spin degrees of freedom factorize [29–36, 57, 58, 61] and the wavefunction of the *lowest lying states* takes the form  $[z = (z_1, \dots, z_N)]$

$$\psi^{\sigma_1 \cdots \sigma_N}(z) = \left[ \sum_{P \in S_N} (-\epsilon)^P P \theta(z) P \chi(\sigma_1, \dots, \sigma_N) \right] \times \psi_F(z|\mathbf{q}^0), \quad (5)$$

with  $\mathbf{q}^0 \equiv (q_1^0, \dots, q_N^0) = (1, \dots, N)$  and

$$\psi_F(z|\mathbf{q}^0) = \frac{1}{\sqrt{N!}} \det_N \left[ \phi_{q_j^0}(z_i) \right]_{i,j=1, \dots, N}, \quad (6)$$

is the Slater determinant formed from the lowest  $N$  orbitals  $\phi_{q_j^0}(z)$  of a system of spinless fermions subjected to the same potential  $V(z)$  and  $\chi(\sigma_1, \dots, \sigma_N)$  is an eigenfunction of a spin chain characterizing the spin degrees of freedom which we will describe below. In Eq. (5)  $\theta(z) \equiv \theta(z_1 < \dots < z_N)$  is a generalized Heaviside function which is 1 when  $z_1 < \dots < z_N$  and zero otherwise and  $S_N$  is the group of permutations of  $N$  elements with  $(-1)^P$  the signature of the permutation. For a given permutation  $P = \begin{pmatrix} 1 & \cdots & N \\ P_1 & \cdots & P_N \end{pmatrix}$  the action of this permutation on  $\theta(z)$  is given by  $P\theta(z) = \theta(z_{P_1} < \dots < z_{P_N})$  and  $P\chi(\sigma_1, \dots, \sigma_N) = \chi(\sigma_{P_1}, \dots, \sigma_{P_N})$ . The spin chain whose wavefunctions describe the spin sector is (we consider the general case with a gradient term) [33–39].

$$H_{sc}^0 = E_F(\mathbf{q}^0) - \frac{1}{g} \sum_{i=1}^{N-1} J_i^0 \left( 1 + \epsilon \hat{P}_{i,i+1} \right) - G \sum_{i=1}^N D_i^0 \sigma_i^z, \quad (7)$$

where  $E_F(\mathbf{q}^0) = \sum_{j=1}^N \epsilon(q_j^0)$  is the groundstate energy of the spinless fermionic system,  $\hat{P}_{i,i+1}$  is the operator that permutes the spins on positions  $i$  and  $i+1$  and  $J_i^0$  are the local exchange coefficients which can be obtained from the Slater determinant  $\psi_F(\mathbf{q}^0)$  via [34]

$$J_i^0 = N! \int dz_1 \cdots dz_N \delta(z_i - z_{i+1}) \theta(z_1 < \dots < z_N) \times \left| \frac{\partial \psi_F(\mathbf{q}^0)}{\partial z_i} \right|^2, \quad i = 1, \dots, N-1. \quad (8)$$

The coefficients  $D_i$  play the role of the average position of the  $i$ -th particle and are given by [33, 35, 37, 38]

$$D_i^0 = N! \int dz_1 \cdots dz_N z_i \theta(z_1 < \dots < z_N) \times |\psi_F(\mathbf{q}^0)|^2, \quad i = 1, \dots, N. \quad (9)$$

The factorization of the wavefunctions (5) simplifies considerably the analytical and numerical investigations of the correlation functions in the strong interacting regime. A major computational hurdle is represented by the fact that the exchange coefficients (8), average positions (9), and, as we will see in the next sections, the one-body density matrix elements (16) and the particle densities (21) require the evaluation of  $(N-1)$  dimensional integrals. The local exchange coefficients for  $N \leq 16$  and harmonic trapping were initially calculated using Monte-Carlo integration or other approximate methods [33–41]. Improved numerical algorithms for arbitrary trapping potentials were introduced in [42, 43] for  $N \leq 35$  and in [44] for  $N \leq 60$ . In the case of harmonic trapping approximate formulae for the local exchange coefficients using the Local Density Approximation can be found in [36, 38] and for the average positions in [38]. While the methods introduced in [43] and [44] present considerable improvements over the previous approaches they require arbitrary precision subroutines and are time consuming for medium and large numbers of particles. In Sec. III we will develop a more efficient method of computing the relevant charge functions.

### B. Excited manifolds and separation of energy scales

The wavefunctions (5) and the spin chain (7) describe the groundstate manifold of states of the strongly interacting spinor gas. In order to investigate the temperature correlators or the dynamics of the system one also needs to consider the excited manifolds. The excited manifolds are constructed in a similar fashion [38] from the excited states of the dual system of spinless fermions, which will be denoted by  $\psi_F(z_1, \dots, z_N|\mathbf{q}^k)$ ,  $k = 1, 2, \dots$ , and the associated spin chain Hamiltonians

$$H_{sc}^k = E_F(\mathbf{q}^k) - \frac{1}{g} \sum_{i=1}^{N-1} J_i^k \left( 1 + \epsilon \hat{P}_{i,i+1} \right) - G \sum_{i=1}^N D_i^k \sigma_i^z, \quad (10)$$



with  $E_F(\mathbf{q}^k)$  being the energies of the fermionic excited states and  $J_i^k$  and  $D_i^k$  having similar definitions as in (8) and (9) but with  $\psi_F(\mathbf{q}^0)$  replaced by  $\psi_F(\mathbf{q}^k)$ . In the case of harmonic trapping the groundstate is  $\psi_F = \psi_F(z_1, \dots, z_N | \mathbf{q}_0)$  with  $\mathbf{q}_0 = (0, 1, \dots, N-1)$  while the first excited state is  $\psi_F(z_1, \dots, z_N | \mathbf{q}_1)$  with  $\mathbf{q}_1 = (0, 1, \dots, N-2, N)$  and  $\phi_j(z)$  the  $j$ -th Hermite function. Their energies are  $E_F(\mathbf{q}^0) = \sum_{j=0}^{N-1} (j+1/2) = N^2/2$  and  $E_F(\mathbf{q}^1) = E_F(\mathbf{q}^0) + 1$ , respectively. For a given sector  $\mathbf{N} = [N_1, \dots, N_\kappa]$  and a free fermionic state  $\mathbf{q}$  there are  $C_{N_1}^N C_{N_2}^{N-N_1} \dots C_{N_{\kappa-1}}^{N-(N_1+N_2+\dots+N_{\kappa-2})} = N!/[N_1! \dots N_\kappa!]$  spin states and we will denote such a state by  $|\Phi_{\mathbf{N}, \mathbf{q}, n}\rangle$  with  $n = 1, \dots, N!/[N_1! \dots N_\kappa!]$ .

The explicit form of the effective Hamiltonians (7) and (10) allows for the investigation of the energy scales of the charge and spin sectors. In the fermionic case the lower bound of the energy for the spin excitations is obtained by considering the fully antisymmetric spin wavefunction  $\chi^a$  which satisfies  $\hat{P}_{i,i+1}\chi^a = -\chi^a$  obtaining  $E_{spin}^{min} = -\frac{2}{g} \sum_{i=1}^{N-1} J_i$ . The upper bound is attained for the fully symmetric spin wavefunction  $\chi^s$  which satisfies  $\hat{P}_{i,i+1}\chi^s = \chi^s$  resulting in  $E_{spin}^{max} = 0$ . A similar result can be derived in the bosonic case but in this case the upper (lower) bound is attained for the fully antisymmetric (symmetric) spin wavefunction. If we denote by  $E(\mathbf{N}, \mathbf{q}^{0,1}, n)$  the energies of the  $|\Phi_{\mathbf{N}, \mathbf{q}^{0,1}, n}\rangle$  eigenstates we have

$$E(\mathbf{N}, \mathbf{q}^0, n) = E_F(\mathbf{q}^0) - \frac{1}{g} E_{spin}(\mathbf{N}, \mathbf{q}^0, n),$$

$$|E_{spin}(\mathbf{N}, \mathbf{q}^0, n)| \in [0, 2 \sum J_i^0], \quad (11)$$

$$E(\mathbf{N}, \mathbf{q}^1, n) = E_F(\mathbf{q}^1) - \frac{1}{g} E_{spin}(\mathbf{N}, \mathbf{q}^1, n),$$

$$|E_{spin}(\mathbf{N}, \mathbf{q}^1, n)| \in [0, 2 \sum J_i^1], \quad (12)$$

where  $E_F(\mathbf{q}^{0,1}) = \sum_{j=1}^N \varepsilon(q_j^{0,1})$  and  $E_{spin}(\mathbf{N}, \mathbf{q}^{0,1}, n)$  are the energies of the spin states. In the strong interaction regime the energy scale of the spin sector  $E_{spin} \sim 1/g$  and the energy scale of the charge sector is  $E_{charge} \equiv E(\mathbf{N}, \mathbf{q}^1, n) - E(\mathbf{N}, \mathbf{q}^0, n) \sim E_F(\mathbf{q}^1) - E_F(\mathbf{q}^0)$  with  $E_{spin} \ll E_{charge}$ . These simple considerations show that if we consider temperatures which are much smaller than the energy difference between the groundstate and the first excited manifold then we can consider the computation of the correlators over only the groundstate manifold as the contribution from the excited manifolds is negligible.

### C. Zero temperature correlators in the strongly interacting regime

One of the main goals of this paper is to derive efficient numerical methods for the field-field correlators of strongly interacting spinor gases at zero and low temperatures. We are particularly interested in studying the transition from the zero temperature regime which is described by LL/bosonization [9, 16] in the fermionic case and the ferromagnetic liquid [18–21] in the bosonic case to the spin incoherent regime [22–28]. We start with the zero temperature correlators. For large but finite repulsion strength the Hamiltonian (7) has a unique groundstate (at  $g = \infty$  all the spin eigenstates are degenerate) and we will denote the groundstate by  $|GS\rangle$ . The field-field correlator for the  $\sigma$  particles at zero temperature, also known as the reduced one-body density matrix, is defined as

$$\rho_\sigma(x, y) = \langle GS | \Psi_\sigma^\dagger(x) \Psi_\sigma(y) | GS \rangle, \quad \sigma = \{1, \dots, \kappa\}. \quad (13)$$

In terms of the wavefunction  $\psi^{\sigma_1 \dots \sigma_N}(z_1, \dots, z_N)$  the field-field correlator can be written as [37]

$$\rho_\sigma(x, y) = \sum_{\sigma_2, \dots, \sigma_N = \{1, \dots, \kappa\}}^{[N_1, \dots, N_{\sigma-1}, \dots, N_\kappa]} \int dz_2 \dots dz_N \bar{\psi}^{\sigma_2 \dots \sigma_N}(x, z_2, \dots, z_N | \mathbf{q}_0) \psi^{\sigma_2 \dots \sigma_N}(y, z_2, \dots, z_N | \mathbf{q}_0), \quad (14)$$

and in the following it will be sufficient to consider only the case  $x \leq y$  because from the previous relation we have  $\rho_\sigma(y, x) = \overline{\rho_\sigma(x, y)}$  with the bar denoting complex conjugation. The factorization of the charge and spin degrees of freedom present in the wavefunction (5) can also be made explicit in the expression for the correlator [37, 44]

$$\rho_\sigma(x, y) = \sum_{d_1=1}^N \sum_{d_2=d_1}^N (-\epsilon)^{d_2+d_1} S_\sigma(d_1, d_2) \rho_{d_1, d_2}(x, y), \quad (15)$$

where

$$\rho_{d_1, d_2}(x, y) = N! \int_{\Gamma_{d_1, d_2}(x, y)} \prod_{\substack{k=1 \\ k \neq d_1}}^N dz_k \bar{\psi}_F(z_1, \dots, z_{d_1-1}, x, z_{d_1+1}, \dots, z_N | \mathbf{q}_0) \psi_F(z_1, \dots, z_{d_1-1}, y, z_{d_1+1}, \dots, z_N | \mathbf{q}_0), \quad (16)$$

with  $\Gamma_{d_1, d_2}(x, y) = L_- \leq z_1 < \dots < z_{d_1-1} < x < z_{d_1+1} < \dots < z_{d_2} < y < z_{d_2+1} < \dots < z_N \leq L_+$ . Here  $L_\pm$  are the boundaries of the system, in the case of harmonic trapping we have  $L_\pm = \pm\infty$  while in the case of Dirichlet boundary conditions  $L_\pm = \pm L/2$ .

While the one-body density matrix elements  $\rho_{d_1, d_2}(x, y)$  are independent on  $\sigma$  the spin functions are defined as

$$S_\sigma(d_1, d_2) = \langle \chi | P_\sigma^{(d_1)}(d_1 \cdots d_2) | \chi \rangle, \quad (17)$$

where  $P_\sigma^{(d_1)} = |\sigma\rangle_{d_1} \langle \sigma|_{d_1}$  is the projector that selects the states that have a  $\sigma$  particle at position  $d_1$  and  $(d_1 \cdots d_2)$  is the permutation that cyclically permutes the spins between the positions  $d_1$  and  $d_2$

$$(d_1 \cdots d_2) = \begin{pmatrix} \cdots & d_1 & d_1 + 1 & \cdots & d_2 - 1 & d_2 & \cdots \\ \cdots & d_2 & d_1 & \cdots & d_2 - 2 & d_2 - 1 & \cdots \end{pmatrix}. \quad (18)$$

From the correlators (13) we can obtain the densities  $\rho_\sigma(x) \equiv \rho_\sigma(x, x)$ , mean occupation numbers  $\rho_\sigma(n) = \int \int \phi_n(x) \phi_n(y) \rho_\sigma(x, y) dx dy$ , and the momentum distributions

$$n_\sigma(k) = \frac{1}{2\pi} \int \int e^{-ik(x-y)} \rho_\sigma(x, y) dx dy. \quad (19)$$

A factorized expression for the densities can be derived from (15) evaluated at  $x = y$  with the result

$$\rho_\sigma(x) = \sum_{d=1}^N S_\sigma(d) \rho_d(x), \quad (20)$$

where

$$\rho_d(x) = N! \int_{\Gamma_d(x)} \prod_{\substack{k=1 \\ k \neq d}}^N dz_k \times |\psi_F(z_1, \dots, z_{d-1}, x, z_{d+1}, \dots, z_N | \mathbf{q}^0)|^2, \quad (21)$$

$\Gamma_d = L_- \leq z_1 < \cdots < z_d < x < z_{d+1} < \cdots < z_N \leq L_+$  and  $S_\sigma(d) = \langle \chi | P_\sigma^{(d)} | \chi \rangle$ . The quantities (21) are called single particle densities and are related to the average positions of the particles (9) via  $D_i^k = \int z \rho_d(z | \mathbf{q}^k) dz$ . Similar to the case of the local exchange coefficients (8) the one-body density matrix elements (16) and single particle densities (21) require the computation of  $(N-1)$ -dimensional integrals over products of Slater determinants which are not easy to evaluate. In addition to Monte-Carlo integration other methods to compute (16) and (21) use Chebyshev interpolation [44] and the connection between the one-body density matrix elements and the correlation functions of impenetrable anyons [47, 48].

#### D. Finite temperature correlators in the strong interacting regime

In order to investigate the transition between the LL/ferromagnetic liquid and SILL regime we will consider the correlation functions at temperatures that are large enough to completely excite the spin sector but smaller than  $E(\mathbf{N}, \mathbf{q}^1, n) - E(\mathbf{N}, \mathbf{q}^0, n) \sim E_F(\mathbf{q}^1) -$

$E_F(\mathbf{q}^0)$  such that only the first manifold of states contribute to the thermal trace (see the discussion in Sec. IIB). We use units of  $k_B = 1$  where  $k_B$  is the Boltzmann constant. In the canonical ensemble the low temperatures correlators in the  $\mathbf{N} = [N_1, \dots, N_\kappa]$  sector are  $[\sigma = \{1, \dots, \kappa\}]$

$$\rho_\sigma^T(x, y) = \sum_{n=1}^{N!/[N_1! \cdots N_\kappa!]} \frac{e^{-E(\mathbf{N}, \mathbf{q}^0, n)/T}}{Z} \times \langle \Phi_{\mathbf{N}, \mathbf{q}^0, n} | \Psi_\sigma^\dagger(x) \Psi_\sigma(y) | \Phi_{\mathbf{N}, \mathbf{q}^0, n} \rangle, \quad (22)$$

with  $Z = \sum_{n=1}^{N!/[N_1! \cdots N_\kappa!]} e^{-E(\mathbf{N}, \mathbf{q}^0, n)/T}$ . In the limit  $T \rightarrow 0$  the finite temperature correlator (22) reduces to (13). At temperatures for which the thermal energy is much larger than the spin energy of the first manifold  $|E_{spin}(\mathbf{N}, \mathbf{q}^0, n)|/g \ll T$  but smaller than the energies of the first excited manifold  $T \ll |E(\mathbf{N}, \mathbf{q}^1, n)|$  we have  $e^{-E(\mathbf{N}, \mathbf{q}^0, n)/T} \sim e^{-E_F(\mathbf{q}^0)/T}$  and (22) becomes

$$\rho_\sigma^{SILL}(x, y) = \sum_{n=1}^{N!/[N_1! \cdots N_\kappa!]} \frac{1}{Z} \times \langle \Phi_{\mathbf{N}, \mathbf{q}^0, n} | \Psi_\sigma^\dagger(x) \Psi_\sigma(y) | \Phi_{\mathbf{N}, \mathbf{q}^0, n} \rangle, \quad (23)$$

with  $Z = N!/[N_1! \cdots N_\kappa!]$  which defines the spin-incoherent Luttinger liquid correlator. It is important to note that while the spin sector is effectively at infinite temperature the charge sector is still in the low temperature regime. All these considerations were made in the case of large but finite repulsion strength. In the limiting case of impenetrable particles  $g = \infty$  all the spin states are degenerate and we can have the system in the SILL regime even at zero temperature [22–25, 28].

### III. EVALUATION OF MULTIDIMENSIONAL INTEGRALS

In this section we are going to develop a new method of evaluating the multidimensional integrals that appear in the definitions of the local exchange coefficients (8), one-body density matrix elements (16) and the single particle densities (21). The main ingredient of our method is the so-called “phase trick” [30, 62, 63] which helps express multidimensional integrals over irregular domains of  $\mathbb{R}^{N-1}$  as Fourier type integrals over determinants of matrices constructed from partial overlaps of the single particle orbitals. The Fourier integrals need to be evaluated only for a discrete set of points task which can be easily accomplished using the Discrete Fourier Transform.

#### A. The single particle densities

The single particle densities are the simplest of the charge functions involving  $N-1$  dimensional integrals.

As we will see their treatment contains all the necessary techniques required to investigate the more complicated functions. We will consider first the case in which the eigenstate is in the groundstate manifold. The generalization for the case of excited manifolds will be presented at the end of the section.

In Appendix A it is shown that the expression for the single particle densities Eq. (21) can be put in a Fourier integral form

$$\rho_d(x) = \int_0^{2\pi} \frac{d\alpha}{2\pi} e^{-i(d-1)\alpha} \int_0^{2\pi} \frac{d\beta}{2\pi} e^{-i\beta} \times \det_N [e^{i\alpha} \mathbf{M}^0 + e^{i\beta} \mathbf{M}^r + \mathbf{M}^1] (x), \quad (24)$$

where  $\mathbf{M}^{0,1,r}(x)$  are three  $N \times N$  matrices with elements

$$[\mathbf{M}^0(x)]_{a,b} = \int_{L_-}^x \bar{\phi}_a(z) \phi_b(z) dz, \quad (25a)$$

$$[\mathbf{M}^1(x)]_{a,b} = \int_x^{L_+} \bar{\phi}_a(z) \phi_b(z) dz, \quad (25b)$$

$$[\mathbf{M}^r(x)]_{a,b} = \bar{\phi}_a(x) \phi_b(x). \quad (25c)$$

This expression can be simplified even further.  $\mathbf{M}^r(x)$  is a rank 1 matrix and can be written as  $\mathbf{M}^r(x) = uv^T$  with  $u = (\bar{\phi}_1(x), \dots, \bar{\phi}_N(x))^T$  and  $v = (\phi_1(x), \dots, \phi_N(x))$ . Now we can use a theorem which states that for an arbitrary matrix  $\mathbf{M}$  and a matrix of rank 1, which can always be written as  $uv^T$  with  $u, v$  arbitrary column vectors, the following identity holds [64]

$$\det(\mathbf{M} + uv^T) = \det \mathbf{M} + v^T \text{adj}(\mathbf{M}) u, \quad (26)$$

with  $\text{adj}(\mathbf{M}) = \det(\mathbf{M}) \mathbf{M}^{-1}$  the adjugate matrix of  $\mathbf{M}$ . Using this identity with  $\mathbf{M} = e^{i\alpha} \mathbf{M}^0 + \mathbf{M}^1$  we obtain  $\det_N (e^{i\alpha} \mathbf{M}^0 + e^{i\beta} \mathbf{M}^r + \mathbf{M}^1) = \det_N \mathbf{M} + e^{i\beta} v^T \text{adj}(\mathbf{M}) u$ . In (24) the integration over  $\beta$  selects the term  $v^T \text{adj}(\mathbf{M}) u$  which is in fact  $\det_N (e^{i\alpha} \mathbf{M}^0 + \mathbf{M}^1 + \mathbf{M}^r) - \det_N (e^{i\alpha} \mathbf{M}^0 + \mathbf{M}^1)$ . Therefore, we find

$$\rho_d(x) = \int_0^{2\pi} \frac{d\alpha}{2\pi} e^{-i(d-1)\alpha} \left[ \det_N (e^{i\alpha} \mathbf{M}^0 + \mathbf{M}^1 + \mathbf{M}^r) - \det_N (e^{i\alpha} \mathbf{M}^0 + \mathbf{M}^1) \right] (x). \quad (27)$$

In the literature there are powerful numerical algorithms [65, 66] to deal with this type of Fourier integrals but we can be more efficient by noticing that we need to compute (27) only for  $d = 1, \dots, N$  for a given  $x$ . Let

$$f(\alpha|x) = \left[ \det_N (e^{i\alpha} \mathbf{M}^0 + \mathbf{M}^1 + \mathbf{M}^r) - \det_N (e^{i\alpha} \mathbf{M}^0 + \mathbf{M}^1) \right] (x), \quad (28)$$

which is a polynomial of order  $N-1$  in  $e^{i\alpha}$  (that it is not of order  $N$  can be seen either from (A3) or using the identity (26) and the fact that the adjugate is the transpose of its cofactor matrix) and can be written as  $f(\alpha|x) =$

$\sum_{n=0}^{N-1} a_n(x) e^{i\alpha n}$  with  $a_n(x) = \rho_{n+1}(x)$ . Computing the coefficients of this polynomial (or, equivalently, the single particle densities) can be done as follows. First, we evaluate  $f_k \equiv f\left(\frac{2\pi k}{N}|x\right) = \sum_{n=0}^{N-1} a_n(x) e^{i\frac{2\pi k}{N}n}$  for  $k = 0, 1, \dots, N-1$ . Having computed the  $N$  vector  $\mathbf{f} \equiv (f_0, \dots, f_{N-1})$  then the coefficients are obtained as

$$a_n(x) \equiv \rho_{n+1}(x) = \frac{1}{N} \sum_{k=0}^{N-1} f_k(x) e^{-i\frac{2\pi n}{N}k}, \quad (29)$$

which is in fact the inverse Discrete Fourier Transform of the vector  $\mathbf{f}$ .

Summarizing, the algorithm for the calculation of the single particle densities (21) is the following: i) compute the matrices  $\mathbf{M}^{0,1,r}(x)$  defined in (25a), (25b) and (25c) (note that in many cases of interest like harmonic trapping, Dirichlet or Neumann boundary conditions the overlaps of single particle orbitals can be analytically computed [54, 67]) and even when this is not the case the numerical evaluation of 1D integrals is moderately computationally expensive); ii) construct the vector  $\mathbf{f}$  by evaluating (28) at  $2\pi k/N, k = 0, 1, \dots, N-1$ ; iii) perform an inverse Discrete Fourier Transform on the vector  $\mathbf{f}$ .

In the case of single particle densities for higher excited manifolds which are described by  $\psi_F(z_1, \dots, z_N|\mathbf{q})$  all the results derived in this section remain valid but in this case the definitions of the  $\mathbf{M}^{0,1,r}$  matrices now become  $[\mathbf{M}^0(x)]_{a,b} = \int_{L_-}^x \bar{\phi}_{q_a}(z) \phi_{q_b}(z) dz$ ,  $[\mathbf{M}^1(x)]_{a,b} = \int_x^{L_+} \bar{\phi}_{q_a}(z) \phi_{q_b}(z) dz$ , and  $[\mathbf{M}^r(x)]_{a,b} = \bar{\phi}_{q_a}(x) \phi_{q_b}(x)$ .

## B. Local exchange coefficients

The computation of the local exchange coefficients (8) follows along the same lines as in the case of single particle densities with the additional complication of dealing with another integration. In Appendix B we show that the expression (8) can be written as

$$J_d^0 = \int_{L_-}^{L_+} I_d(\xi) d\xi, \quad (30)$$

with

$$I_d(\xi) = \int_0^{2\pi} \frac{d\alpha}{2\pi} e^{-i(d-1)\alpha} \int_0^{2\pi} \frac{d\beta}{2\pi} e^{-i\beta} \int_0^{2\pi} \frac{d\gamma}{2\pi} e^{-i\gamma} \times \det_N [e^{i\alpha} \mathbf{M}^0 + e^{i\beta} \mathbf{M}^r + e^{i\gamma} \mathbf{M}^d + \mathbf{M}^1] (\xi). \quad (31)$$

We introduced a new  $N \times N$  matrix defined by  $[\phi'_a(\xi)]$  is the derivative of  $\phi_a(\xi)$

$$[\mathbf{M}^d(\xi)]_{a,b} = \bar{\phi}'_a(\xi) \phi'_b(\xi), \quad (32)$$

and the matrices  $\mathbf{M}^{0,1,r}(\xi)$  are defined in (25a), (25b), (25c). Both  $\mathbf{M}^d(\xi)$  and  $\mathbf{M}^r(\xi)$  are rank 1 matrices and the integrations over  $\beta$  and  $\gamma$  can be eliminated like in Sec. III A by using the identity (26) twice obtaining

$$I_d(\xi) = \int_0^{2\pi} \frac{d\alpha}{2\pi} e^{-i(d-1)\alpha} \left[ \det_N \left( e^{i\alpha} \mathbf{M}^0 + \mathbf{M}^1 + \mathbf{M}^r + \mathbf{M}^d \right) - \det_N \left( e^{i\alpha} \mathbf{M}^0 + \mathbf{M}^1 + \mathbf{M}^d \right) - \det_N \left( e^{i\alpha} \mathbf{M}^0 + \mathbf{M}^1 + \mathbf{M}^r \right) - \det_N \left( e^{i\alpha} \mathbf{M}^0 + \mathbf{M}^1 \right) \right] (\xi). \quad (33)$$

Like in the previous section we do not need to compute the integral to obtain  $I_d(\xi)$ . Let

$$g(\alpha|\xi) = \left[ \det_N \left( e^{i\alpha} \mathbf{M}^0 + \mathbf{M}^1 + \mathbf{M}^r + \mathbf{M}^d \right) - \det_N \left( e^{i\alpha} \mathbf{M}^0 + \mathbf{M}^1 + \mathbf{M}^d \right) - \det_N \left( e^{i\alpha} \mathbf{M}^0 + \mathbf{M}^1 + \mathbf{M}^r \right) - \det_N \left( e^{i\alpha} \mathbf{M}^0 + \mathbf{M}^1 \right) \right] (\xi), \quad (34)$$

which is a polynomial of order  $N-2$  in  $e^{i\alpha}$  i.e  $g(\alpha, \xi) = \sum_{n=0}^{N-2} b_n(\xi) e^{in\alpha}$  with  $b_n(\xi) = I_{n+1}(\xi)$ . Introducing the vector  $\mathbf{g}(\xi) = (g_0(\xi), \dots, g_{N-1}(\xi))$  with elements  $g_k(\xi) \equiv g(\frac{2\pi k}{N}|\xi) = \sum_{n=0}^{N-1} b_n(\xi) e^{i\frac{2\pi k}{N}n}$  then the  $I_n(\xi)$  are obtained as the inverse Discrete Fourier Transform of  $\mathbf{g}(\xi)$

$$b_n(\xi) \equiv I_{n+1}(\xi) = \frac{1}{N} \sum_{k=0}^{N-1} g_k(\xi) e^{-i\frac{2\pi n}{N}k}. \quad (35)$$

The algorithm for computing the local exchange coefficients is as follows: i) approximate the integral (30) with an  $M$ -point quadrature (Chap. IV of [68])

$$J_d^0 = \int_{L_-}^{L_+} I_d(\xi) d\xi \sim \sum_{j=1}^M I_d(\xi_j) w_j, \quad (36)$$

where  $\xi_j$  and  $w_j$ ,  $j = 1, \dots, M$  are the abscissas and the weights of the quadrature; ii) for each value of the abscissas  $\xi_j$  compute the matrices  $\mathbf{M}^{0,1,r,d}(\xi_j)$  defined in (25a), (25b), (25c) and (32); iii) compute the vectors

$\mathbf{g}(\xi_j) = (g_0(\xi_j), \dots, g_{N-1}(\xi_j))$  for each  $\xi_j$ ; iv) perform a Discrete Fourier Transform on the vectors  $\mathbf{g}(\xi_j)$  to obtain  $I_d(\xi_j)$ ,  $d = 1, \dots, N-1$  for each  $\xi_j$ ; v) do the summation in (36).

The generalization for the case of local exchange coefficients of the higher excited manifolds which are described by  $\psi_F(z_1, \dots, z_N|\mathbf{q})$  is obtained by changing the definition of the matrices  $\mathbf{M}^{0,1,r,d}(\xi)$  to  $[\mathbf{M}^0(x)]_{a,b} = \int_{L_-}^x \bar{\phi}_{q_a}(z) \phi_{q_b}(z) dz$ ,  $[\mathbf{M}^1(x)]_{a,b} = \int_x^{L_+} \bar{\phi}_{q_a}(z) \phi_{q_b}(z) dz$ ,  $[\mathbf{M}^r(x)]_{a,b} = \bar{\phi}_{q_a}(x) \phi_{q_b}(x)$  and  $[\mathbf{M}^d(\xi)]_{a,b} = \bar{\phi}'_{q_a}(\xi) \phi'_{q_b}(\xi)$ .

### C. The one-body density matrix elements

The computation of the one-body density matrix elements (16) presents some particularities compared to the case of the local exchange coefficients or the average positions of particles. We will only need to consider the case  $x \leq y$  due to the fact that  $\rho_\sigma(x, y) = \rho_\sigma(y, x)$ . In Appendix C it is shown that (16) is equivalent to the following Fourier integral expression

$$\rho_{d_1, d_2}(x, y) = \int_0^{2\pi} \frac{d\alpha}{2\pi} e^{-i(d_1-1)\alpha} \int_0^{2\pi} \frac{d\gamma}{2\pi} e^{-i\gamma} \int_0^{2\pi} \frac{d\beta}{2\pi} e^{-i(d_2-d_1)\beta} \det_N [e^{i\alpha} \mathbf{M}^0 + e^{i\gamma} \mathbf{M}^n + e^{i\beta} \mathbf{M}^2 + \mathbf{M}^1] (x, y), \quad (37)$$

where in addition to  $\mathbf{M}^{0,1}$  defined in (25a), (25b) we have introduced two  $N \times N$  matrices with elements

$$[\mathbf{M}^2(x, y)]_{a,b} = \int_x^y \bar{\phi}_a(z) \phi_b(z) dz, \quad (38a)$$

$$[\mathbf{M}^n(x, y)]_{a,b} = \bar{\phi}_a(x) \phi_b(y). \quad (38b)$$

The matrix  $\mathbf{M}^n$  is of rank 1 so we can use the identity (26) to integrate over  $\gamma$  obtaining

$$\rho_{d_1, d_2}(x, y) = \int_0^{2\pi} \frac{d\alpha}{2\pi} e^{-i(d_1-1)\alpha} \int_0^{2\pi} \frac{d\beta}{2\pi} e^{-i(d_2-d_1)\beta}$$

$$\times \left[ \det_N (e^{i\alpha} \mathbf{M}^0 + e^{i\beta} \mathbf{M}^2 + \mathbf{M}^1 + \mathbf{M}^n) - \det_N (e^{i\alpha} \mathbf{M}^0 + e^{i\beta} \mathbf{M}^2 + \mathbf{M}^1) \right] (x, y). \quad (39)$$

Compared with the previous cases now we have a double integral. Let

$$h(\alpha, \beta|x, y) = \left[ \det_N (e^{i\alpha} \mathbf{M}^0 + e^{i\beta} \mathbf{M}^2 + \mathbf{M}^1 + \mathbf{M}^n) - \det_N (e^{i\alpha} \mathbf{M}^0 + e^{i\beta} \mathbf{M}^2 + \mathbf{M}^1) \right] (x, y). \quad (40)$$



TABLE I. Evaluation times (in seconds) of the local exchange coefficients  $J_i$  [Eq. (8)], single particle densities  $\rho_d(x)$  [Eq. (21)] and one-body density matrix elements  $\rho_{d_1,d_2}(x,y)$  [Eq. (16)] computed using the approach of this paper and the method described in [44].

$N$	$J_i$		$\rho_d(x)$		$\rho_{d_1,d_2}(x,y)$	
	Sec. III B	Deuretzbacher <i>et al.</i> [44]	Sec. III A	Deuretzbacher <i>et al.</i> [44]	Sec. III C	Deuretzbacher <i>et al.</i> [44]
5	0.07365	1.07895	0.00035	0.05158	0.00139	0.16181
10	0.08448	3.01429	0.00056	0.12947	0.00261	2.08619
15	0.09863	12.7829	0.00094	0.31709	0.00608	14.4611
20	0.11728	364.804	0.00150	4.24389	0.01523	742.804
30	0.28917	3327.92	0.00410	35.6766	0.05876	—
60	1.55943	— <sup>a</sup>	0.01854	—	0.77707	—
120	28.8309	—	0.12357	—	12.3981	—

<sup>a</sup> In the code from the arXiv version of [44] an evaluation time of 853895 seconds for  $N = 60$  is reported for an unspecified 4 core CPU.

As a multivariate polynomial in  $e^{i\alpha}$  and  $e^{i\beta}$  the maximum degree term appearing in the expansion of  $h(\alpha, \beta|x, y)$  is  $e^{in_1\alpha}e^{in_2\beta}$  with  $n_1 + n_2 = N - 1$  (this can be seen from (C3)). We have

$$h(\alpha, \beta|x, y) = \sum_{n_1=0}^{N-1} \sum_{n_2=0}^{N-1} c_{n_1,n_2}(x, y) e^{i\alpha n_1} e^{i\beta n_2}, \quad (41)$$

with  $c_{n_1,n_2}(x, y) = 0$  if  $n_1 + n_2 > N - 1$ . Because  $c_{d_1-1,d_2-d_1}(x, y) = \rho_{d_1,d_2}(x, y)$  ( $d_1, d_2 = 1, \dots, N$ ) this shows that  $\rho_{d_1,d_2}(x, y)$  is an upper triangular matrix i.e.,  $\rho_{d_1,d_2}(x, y) = 0$  for  $d_1 < d_2$ . Introducing the  $N \times N$  matrix  $\mathbf{h}(x, y)$  with elements  $(k_1, k_2 = 0, \dots, N - 1)$

$$\mathbf{h}_{k_1,k_2}(x, y) = h\left(\frac{2\pi k_1}{N}, \frac{2\pi k_2}{N}|x, y\right), \quad (42)$$

then the  $c_{n_1,n_2}$  coefficients, or, equivalently, the one-body density matrix elements can be obtained via a 2D Discrete Fourier Transform

$$c_{n_1,n_2}(x, y) = \frac{1}{N^2} \sum_{k_1=0}^{N-1} \left[ e^{-i\frac{2\pi n_1}{N}k_1} \times \sum_{k_2=0}^{N-1} e^{-i\frac{2\pi n_2}{N}k_2} \mathbf{h}_{k_1,k_2}(x, y) \right]. \quad (43)$$

Therefore, the algorithm for the calculation of the one-body density matrix elements is the following: i) for given  $x$  and  $y$  satisfying  $x \leq y$  compute the matrices  $\mathbf{M}^{0,1,2,n}$  defined in (25a), (25b), (38a) and (38b); ii) compute the matrix  $\mathbf{h}(x, y)$  defined in (42); iii) the one-body density matrix elements are obtained by performing a 2D inverse Discrete Fourier Transform on the matrix  $\mathbf{h}(x, y)$ . In the case of an excited manifold described by  $\psi_F(z_1, \dots, z_N|\mathbf{q})$  one needs to modify the definition of the matrices  $\mathbf{M}^{0,1,2,n}$  to  $[\mathbf{M}^0(x)]_{a,b} = \int_{L_-}^x \bar{\phi}_{q_a}(z) \phi_{q_b}(z) dz$ ,  $[\mathbf{M}^2(x, y)]_{a,b} = \int_x^y \bar{\phi}_{q_a}(z) \phi_{q_b}(z) dz$  and so on.

## D. Comparison with other approaches

The algorithms introduced in the previous sections are extremely simple, exact, numerically stable, and do not require the use of arbitrary precision subroutines. The computation of the auxiliary quantities like the overlap matrices, the determinants and the Discrete Fourier Transforms can be done very efficiently using well known techniques [68]. In Table I we present the evaluation times of the local exchange coefficients, single particle densities and the one-body density matrix elements for harmonically trapped systems with different number of particles ranging from  $N = 5$  to  $N = 120$  computed using the method introduced in this paper compared with the results obtained by running the code provided in the arXiv version of [44]. The results reported were computed using an AMD processor (Ryzen 9 5900HX at 3.30GHz with 8 cores) and 64 GB of RAM using the same interpreted language as in [44]. In order to simulate the case of an arbitrary potential we have calculated the overlap matrices using the Clenshaw-Curtis quadrature with 10 to 20 points per unit of harmonic oscillator length  $l_o = \sqrt{\hbar/(m\omega)}$ . For all values of  $N$  and especially for medium and large number of particles our method significantly outperforms the approach of [44]. This statement is also true in the case of the method introduced in [43] in which the authors report that the calculation of the local exchange coefficients on an Intel Xenon processor (E5-2630 v3 at 2.40GHz with 8 cores) for  $N = 10$  takes approximately 10 seconds, for  $N = 20$  less than 10 minutes and about an hour for  $N = 30$ . The one-body density matrix elements can also be evaluated using the method introduced in [47]. In the general case it requires the computation of  $\sim N^4$  overlap integrals of anyonic type and  $\sim N^4$  determinants of  $N \times N$  matrices. Our method requires only  $\sim N^2$  integrals and  $\sim N^2$  determinants which represents a large polynomial improvement in numerical efficiency.

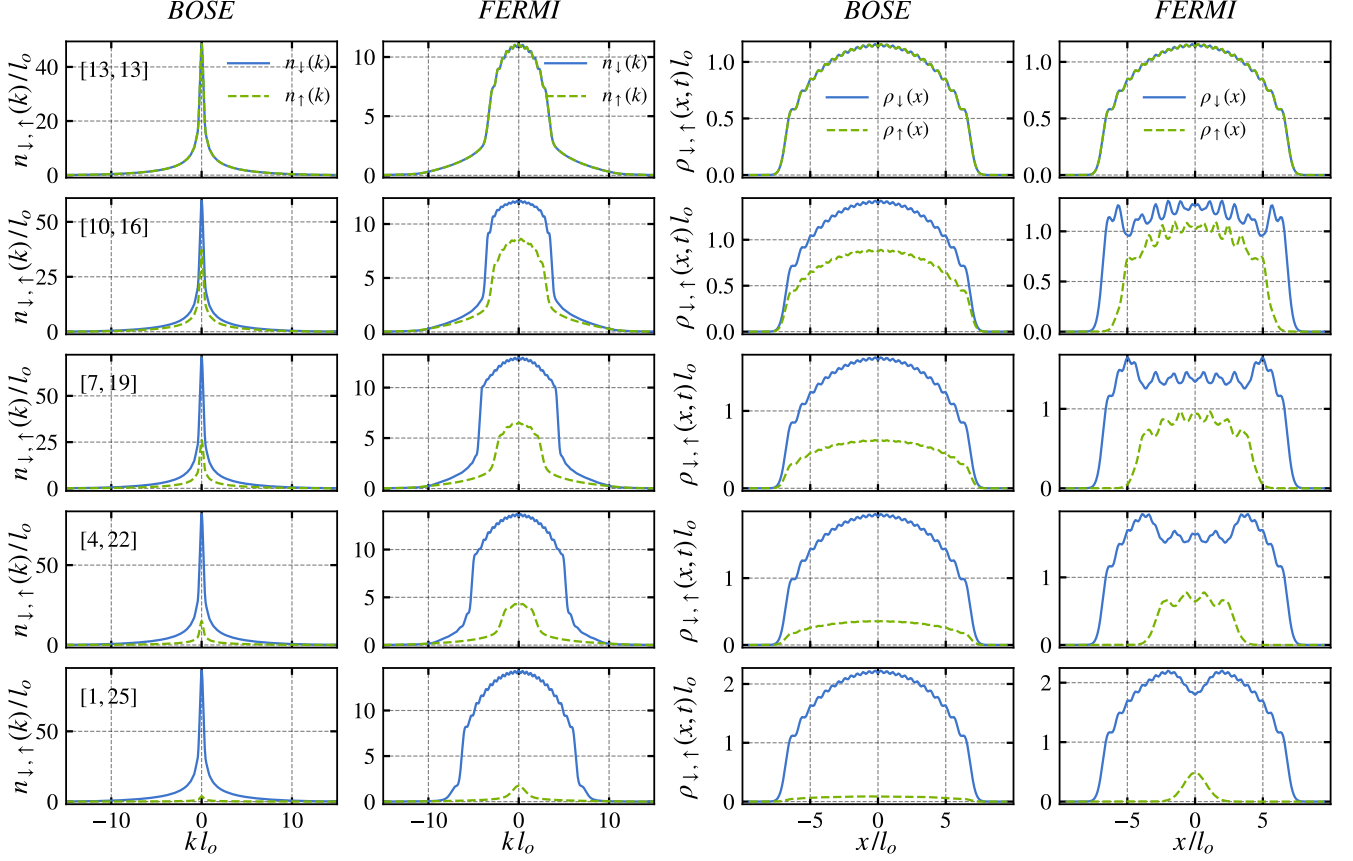


FIG. 1. Momentum distributions (first and second column) and densities (third and fourth columns) in the groundstates of harmonically trapped two-component bosons and fermions with  $N = 26$  and different values of population imbalance. First row  $[N_{\uparrow}, N_{\downarrow}] = [13, 13]$ , second row  $[N_{\uparrow}, N_{\downarrow}] = [10, 16]$ , third row  $[N_{\uparrow}, N_{\downarrow}] = [7, 19]$ , fourth row  $[N_{\uparrow}, N_{\downarrow}] = [4, 22]$  and fifth row  $[N_{\uparrow}, N_{\downarrow}] = [1, 25]$ . The relevant parameters are  $m = \omega = 1, g = 100$  ( $l_o$  is the harmonic oscillator length).

#### IV. NUMERICAL RESULTS

The method introduced in the previous section substantially reduce the computation time of the correlators allowing for the investigation of systems with a larger number of particles than before. In Fig. 1 we present results for the densities and momentum distributions of a harmonically trapped two-component system of  $N = 26$  particles with  $g = 100$  and different values of the population imbalance. We mention that the computational limitation in this case comes from the exact diagonalization of the effective spin chain (7) with  $D_i^0 = 0$  which in the balanced sector  $N_{\downarrow} = N_{\uparrow} = 13$  has dimension  $C_{13}^{26} = 10400600$ . Employing another method, like DMRG, for the calculation of the spin functions  $S_{\sigma}(d_1, d_2)$  (17) one could in principle study systems with up to 100 particles. In the balanced case the densities are the same for both statistics and are very close to the one for noninteracting spinless fermions  $\rho_{\sigma}(x) \sim \frac{1}{2}\rho_{FF}(x)$  with  $\rho_{FF}(x) = \frac{1}{2}\sum_{j=0}^N |\phi_j(x)|^2$ . As functions of the population imbalance the bosonic densities satisfy  $\rho_{\sigma}(x) \sim (N_{\sigma}/N)\rho_{FF}(x)$  (third column of

Fig. 1) while in the fermionic case the density profiles reorganize such that the spin-up and spin-down parts avoid overlapping [32]. While the overall shape of the total density profiles (ignoring the small oscillations) can be obtained using the Thomas-Fermi approximation, this approach does not produce the correct density profiles of individual components in the fermionic case.

The momentum distributions for bosons have the characteristic shape of a quasicondensate with a large number of particles with momenta close to  $k = 0$  while in the case of fermions they are similar to the momentum distribution of spinless noninteracting fermions above a flat background [44]. Some of the previous numerical investigations of the momentum distribution for trapped and homogeneous multicomponent systems can be found in [29, 37, 40, 41, 44, 48, 51, 59–61, 69]. A distinctive feature of the fermionic distribution is the presence of small oscillations with the number of maxima equaling the number of particles in each component. In both cases the momentum distributions have wide tails and for large values of  $k$  they behave like  $\lim_{k \rightarrow \infty} n_{\sigma}(k) \sim C_{\sigma}/k^4$  with  $C_{\sigma}$  the Tan contacts [70–76]. The  $1/k^4$  tail is an univer-

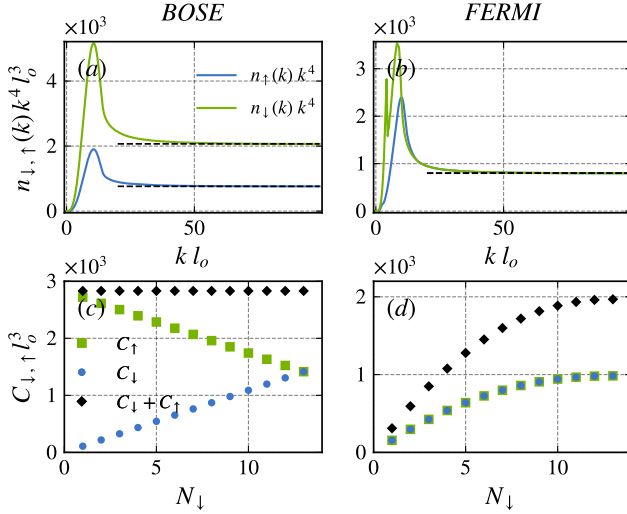


FIG. 2. Scaled momentum distributions  $n_{\uparrow,\downarrow}(k)k^4$  for the groundstate of harmonically trapped bosons a) and fermions b) with  $[N_{\uparrow}, N_{\downarrow}] = [7, 19]$  and  $m = \omega = 1, g = 100$ . The dashed black lines represent the values of the contacts  $C_{\uparrow,\downarrow}$ . Dependence of the contacts on population imbalance for a system of harmonically trapped bosons c) and fermions d) with  $N = 26$ .

sal feature of systems with contact interactions and the contacts are experimentally measurable. While the total contact  $C = \sum_{\sigma=1}^{\kappa} C_{\sigma}$  can be obtained from the ground-state energy of the spin chain (7) the contacts for each component need to be computed using other methods. In Fig. 2c) and 2d) we present the dependence on population imbalance of the contacts for each component,  $C_{\sigma}$ , and total contact,  $C$ , for a trapped two-component system with  $N = 26$ . The contacts are obtained by fitting the tails of the momentum distributions [see Fig. 2a) and 2b)]. In the bosonic case  $C$  is independent of imbalance but the individual contacts increase and decrease linearly as a function of  $N_{\downarrow}$ . This is to be expected when we take into account that we consider the inter- and intra-particle interactions to be equal and that the contacts are directly proportional with the interaction energy. In the fermionic case the individual contacts are equal, for an analytical proof see [75, 76], and they are a monotonically increasing, but not linearly, function of  $N_{\downarrow}$  with the maximum attained for the balanced system. For the same value of imbalance the total contact of the bosonic system is larger than the fermionic one resulting in a wider momentum distribution in the tails.

The role of the temperature in strongly interacting spinor gases has not been sufficiently explored in the literature. This is a rather remarkable oversight when we take into account that strongly interacting systems with internal degrees of freedom present two temperature scales and small changes in the temperature can be accompanied by dramatic changes in their static and dynamic properties [28, 49]. We investigate first the de-

pendence on temperature of the momentum distribution using Eq. (22) for the correlators. We consider temperatures ranging from zero to  $E_{\text{spin}} \ll T \ll E_{\text{charge}}$  that cover the transition from the LL/ferromagnetic liquid phase to the SILL regime. In Fig. 3 we present the temperature dependence of the momentum distribution for balanced harmonically trapped systems with strong interactions,  $g = 10000$ , and  $\kappa = \{2, 3, 4\}$ . For the largest temperature considered  $T = 0.1\omega$  all the systems are in the SILL regime as the spin sector is almost completely excited. We see that as the temperature is increased, contrary to the usual expectations, the number of particles at high momenta decreases, feature which is best exemplified by the monotonically decreasing contacts (see the insets in the second and fourth column of Fig. 3). This momentum reconstruction is accompanied by a decrease of the number of particles at momenta close to zero and an increase in the number of particles at intermediate momenta. This remarkable phenomenon is within reach of current ultracold gases experiments [8, 77] and was predicted for two-component systems [49–51]. Here, in addition to mapping the entire transition, we show that it is present in systems with more than two components being a general feature of multicomponent systems. In [51] it was argued that the minimum of the contact is due to the mixing of states with different exchange symmetries and we expect that the amplitude of the reconstruction to decrease as the number of components becomes large. At higher temperatures, when the charge sector also becomes excited, the contacts and the tails behave conventionally increasing with temperature [60].

Small changes in temperature can also produce impressive changes in the transport properties of strongly interacting spinor gases. In Fig. 4 we present the time dependence of the integrated magnetization

$$M_z(t) = \int_0^{\infty} [\rho_{\downarrow}(z, t) - \rho_{\uparrow}(z, t)] - [\rho_{\downarrow}(z, 0) - \rho_{\uparrow}(z, 0)] dz, \quad (44)$$

after a quench from a domain wall like state for several values of the temperature. We consider a balanced fermionic system with  $N = 16$  particles initially prepared in an thermal state of (7) with a strong gradient  $G$  which results in spin segregation as it can be seen in the first column of Fig. 4. At  $t = 0$  we quench the gradient to zero and let the system evolve. At zero temperature this nonequilibrium scenario was previously investigated in [37, 38, 52]. After the quench the momentum distribution remains almost unchanged (oscillations would be produced if one would consider a spinor gas with different inter- and intra-particles couplings like [78] which would break the  $SU(2)$  symmetry, see also the discussion in [79]) but the integrated magnetization presents oscillatory dynamics at large times [52]. At zero temperature and immediately after the quench the integrated magnetization presents superdiffusive behaviour [52, 80] with  $M_z(t) \sim t^{0.62}$ . The extremely sensitive nature on temperature of the transport properties for multicomponent systems can be seen in the second column of Fig. 4. Even

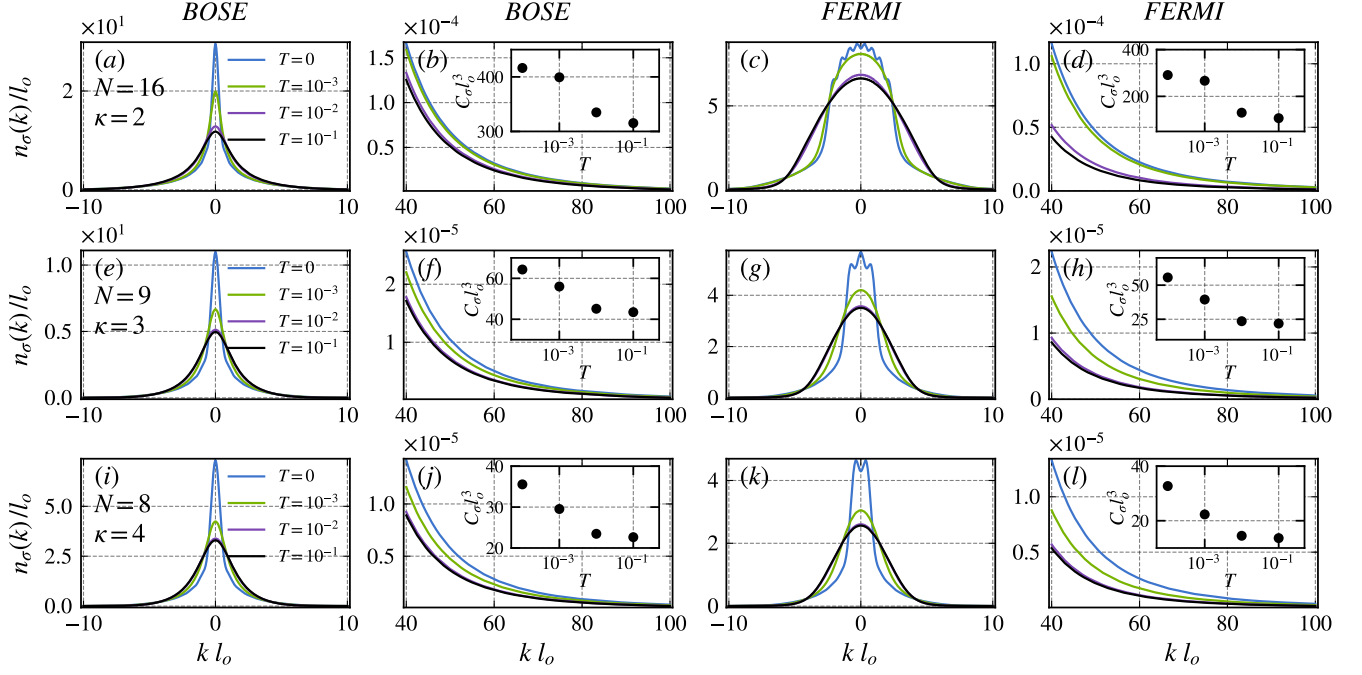


FIG. 3. Dependence on temperature of the momentum distribution for balanced harmonically trapped systems ( $m = \omega = 1, g = 10000$ ) with  $N = 16, \kappa = 2$  (first row),  $N = 9, \kappa = 3$  (second row) and  $N = 8, \kappa = 4$  (third row). The second and fourth column contains zooms of the right tails of the momentum distributions in the interval  $k \in [40, 100]$  with the insets depicting the Tan contacts computed at  $T = \{10^{-4}, 10^{-3}, 10^{-2}, 10^{-1}\} \times \omega$ . The values of the contacts at  $T = 10^{-4}\omega$  are almost indistinguishable from the zero temperature contacts.

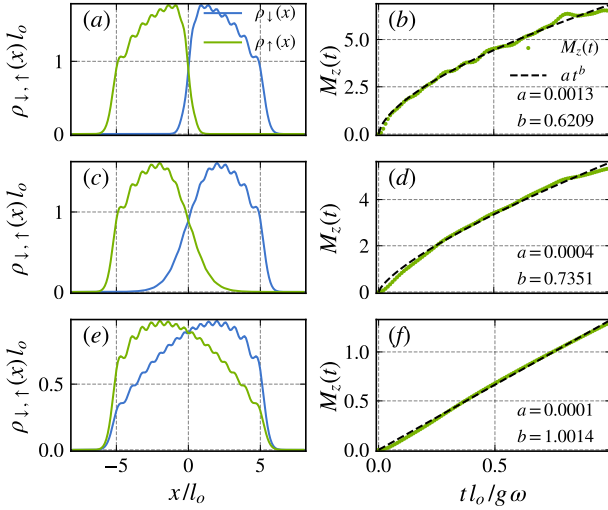


FIG. 4. Time and temperature dependence (first row  $T = 0$ , second row  $T = 0.01\omega$  and third row  $T = 0.1\omega$ ) of the integrated magnetization  $M_z(t)$  for a balanced two-component fermionic system with  $N = 16$  particles after a quench from a domain wall like state. The parameters of the initial Hamiltonian (7) are  $G = 0.014, g = 10000$  and  $m = \omega = 1$ . In the first column we present the initial densities at  $t = 0$  and in the second column  $M_z(t)$  (continuous green line) and the best fit obtained for  $a t^b$  (dashed black line) with  $a$  and  $b$  free parameters.

minute changes in temperature, for which the charge degrees of freedom remain effectively frozen, produce ballistic transport  $M_z(t) \sim t^{1.001}$  as it can be seen in Fig. 4f). This result is particularly intriguing because in the case of the homogeneous Hubbard model, which can be understood as the lattice counterpart of the fermionic two-component spinor gas, it was observed [81] that after a quench from a thermal state at *infinite* temperature with a weak imbalance in the magnetization the spin current presents Kardar-Parisi-Zhang scaling [82] implying  $M_z(t) \sim t^{2/3}$ .

## V. DETERMINANT REPRESENTATIONS FOR THE TRAPPED SILL CORRELATORS

In the spin incoherent regime the factorized nature of the mean value of bilocal operators  $\langle \Phi_{\mathbf{N}, \mathbf{q}, n} | \Psi_{\sigma}^{\dagger}(x) \Psi_{\sigma}(y) | \Phi_{\mathbf{N}, \mathbf{q}, n} \rangle$  and the method employed in Sec. III C to compute the one-body density matrix elements can be used to derive determinant representations for the SILL correlators at zero and finite temperature. In this section we will consider the case of impenetrable particles,  $g = \infty$ , but our results are also true in the case of large and finite coupling strength if the thermal energy is much larger than the

energy of the spin sector  $E_{spin}/g \ll T$ . When doing numerics at finite temperature, like in Sec. IV, it was preferable to use the canonical ensemble (22) but in this section, focused on analytical derivations, it will be more useful to use the grandcanonical ensemble.

In the grandcanonical ensemble at temperature  $T$  and chemical potentials  $\mu_1, \dots, \mu_\kappa$  an explicit expression for the field-field correlator in the SILL regime is given by (here we consider the sum over all the excited manifolds)

$$\rho_\sigma(x, y) = \frac{1}{Z} \sum_{N=0}^{\infty} \sum_{q_1 < \dots < q_N} \sum_{N_1=0}^N \sum_{N_2=0}^{N-N_1} \dots \sum_{N_{\kappa-1}=0}^{N-(N_1+\dots+N_{\kappa-2})} \sum_{n=1}^{N!/[N_1! \dots N_\kappa!]} \times e^{-\sum_{j=1}^N \varepsilon(q_j)/T + \sum_{\sigma'=1}^{\kappa} \mu_{\sigma'} N_{\sigma'}/T} \langle \Phi_{\mathbf{N}, \mathbf{q}, n} | \Psi_\sigma^\dagger(x) \Psi_\sigma(y) | \Phi_{\mathbf{N}, \mathbf{q}, n} \rangle \quad (45)$$

with  $Z$  the grandcanonical partition function (see Appendix D),  $\mathbf{N} = [N_1, \dots, N_\kappa]$  with  $\sum_{j=1}^{\kappa} N_j = N$  and  $\mathbf{q} = (q_1, \dots, q_N)$ . For a given  $\mathbf{N}$  and  $\mathbf{q}$  there are  $N!/[N_1! \dots N_\kappa!]$  spin eigenstates which are indexed by the subscript  $n$  in  $|\Phi_{\mathbf{N}, \mathbf{q}, n}\rangle$ . The statistical contribution of a spin state is  $e^{-E_{spin}(\mathbf{N}, \mathbf{q}, n)/gT}$  and because we consider  $g = \infty$  or temperatures  $E_{spin}/g \ll T$  these factors are effectively equal to 1. Each mean value of the bilocal operators  $\langle \Phi_{\mathbf{N}, \mathbf{q}, n} | \Psi_\sigma^\dagger(x) \Psi_\sigma(y) | \Phi_{\mathbf{N}, \mathbf{q}, n} \rangle$  appearing in (45) can be written in a charge and spin factorized form like (15) with the result

$$\rho_\sigma(x, y) = \frac{1}{Z} \sum_{N=0}^{\infty} \sum_{q_1 < \dots < q_N} \sum_{d_1=1}^N \sum_{d_2=d_1}^N (-\epsilon)^{d_1+d_2} e^{-\sum_{j=1}^N \varepsilon(q_j)/T} \rho_{d_1, d_2}(x, y | \mathbf{q}) S_\sigma^{SILL}(d_1, d_2), \quad (46)$$

where

$$S_\sigma^{SILL}(d_1, d_2) = \sum_{N_1=0}^N \sum_{N_2=0}^{N-N_1} \dots \sum_{N_{\kappa-1}=0}^{N-(N_1+\dots+N_{\kappa-2})} \sum_{n=1}^{N!/[N_1! \dots N_\kappa!]} e^{\sum_{\sigma'=1}^{\kappa} \mu_{\sigma'} N_{\sigma'}/T} \langle \chi_{\mathbf{N}, n} | P_\sigma^{(d_1)}(d_1 \dots d_2) | \chi_{\mathbf{N}, n} \rangle. \quad (47)$$

In (46)  $\rho_{d_1, d_2}(x, y | \mathbf{q})$  is the generalization of Eq. (16) in the case of an excited manifold described by  $\mathbf{q}$ . Both  $\rho_{d_1, d_2}(x, y | \mathbf{q})$  and  $S_\sigma^{SILL}(d_1, d_2)$  depend on  $N$  but we will not make explicit this dependence in order to keep the notation light. Even though (46) and (47) seem daunting we will show below that they reduce to very simple determinant representations which are easily implementable numerically and can also be used to derive rigorous analytical results.

#### A. Computation of $S_\sigma^{SILL}$

The spin function  $S_\sigma^{SILL}(d_1, d_2)$  defined above can be understood as the trace of an operator in the Hilbert space of a spin chain with  $N$  lattice sites and spin  $s = (\kappa - 1)/2$

$$S_\sigma^{SILL}(d_1, d_2) = \text{Tr} \left[ e^{\sum_{\sigma'=1}^{\kappa} \mu_{\sigma'} \hat{N}_{\sigma'}/T} P_\sigma^{(d_1)}(d_1 \dots d_2) \right]. \quad (48)$$

Because the trace is invariant to a change of basis it is preferable to use the canonical basis  $|\sigma_1 \sigma_2 \dots \sigma_N\rangle$  with  $\sigma_i \in \{1, \dots, \kappa\}$ . For a particular  $\kappa$  the cardinality of the basis is  $\kappa^N$ . The effect of the operator  $e^{\mu_{\sigma'} \hat{N}_{\sigma'}/T}$  on any element of the basis is simple producing a multiplicative

factor  $e^{\mu_{\sigma'}/T}$  for any element in  $|\sigma_1 \sigma_2 \dots \sigma_N\rangle$  which is  $\sigma'$ . The operator  $P_\sigma^{(d_1)}(d_1 \dots d_2)$  acting on the basis selects the vectors that have a particle of type  $\sigma$  on position  $d_1$  after a cyclic permutation of the spins between the positions  $d_1$  and  $d_2$ . Therefore, the only vectors of the basis that give a nonzero contribution to the trace are those that have spins of type  $\sigma$  between the  $d_1$  and  $d_2$  positions [48]. Let us consider the three-component case  $\kappa = 3$  and  $\sigma = 1$ . The basis elements that have only  $l = d_2 - d_1 + 1$  spins of type  $\sigma$ , all of them between the positions  $d_1$  and  $d_2$ , produce a term  $C_0^{N-l} e^{\mu_1 l/T} \left( \sum_{k=0}^{N-l} C_k^{N-l} e^{\mu_2 k/T} e^{\mu_3 (N-k-l)/T} \right)$  while the basis elements that have  $l+1$  spins of type  $\sigma$  ( $l$  of them between  $d_1$  and  $d_2$ ) give a contribution  $C_1^{N-l} e^{\mu_1 (l+1)/T} \left( \sum_{k=0}^{N-l-1} C_k^{N-l-1} e^{\mu_2 k/T} e^{\mu_3 (N-k-l-1)/T} \right)$  and so on. Summing all these contributions and using the binomial theorem we obtain  $S_1^{SILL}(d_1, d_2) = e^{\mu_1 l/T} (e^{\mu_1/T} + e^{\mu_2/T} + e^{\mu_3/T})^{N-l}$ . The obvious generalization for arbitrary  $\kappa$  and  $\sigma$  is

$$S_\sigma^{SILL}(d_1, d_2) = \left( \frac{e^{\mu_\sigma/T}}{e^{\mu_1/T} + \dots + e^{\mu_\kappa/T}} \right)^{d_2-d_1+1} \times \left( e^{\mu_1/T} + \dots + e^{\mu_\kappa/T} \right)^N. \quad (49)$$



### B. Large $N$ limit of the correlators

The correlator (46) can also be written as

$$\rho_\sigma(x, y) = \frac{1}{Z} \sum_{N=0}^{\infty} \sum_{q_1 < \dots < q_N} \sum_{d_1=1}^N \sum_{d_2=d_1}^N A_\sigma(d_1, d_2 | \mathbf{q}), \quad (50)$$

with

$$A_\sigma(d_1, d_2 | \mathbf{q}) = (-\epsilon)^{d_2-d_1} e^{-\sum_{j=1}^N \epsilon(q_j)/T} \times \rho_{d_1, d_2}(x, y | \mathbf{q}) S_\sigma^{SILL}(d_1, d_2). \quad (51)$$

The next step in our analysis will take advantage of the extremely simple form of  $S_\sigma^{SILL}(d_1, d_2)$  (49) which can be used to derive a formula similar to (39) for  $A_\sigma(d_1, d_2 | \mathbf{q})$ . We can do this because by multiplying a matrix appearing in (39) with a constant  $c$  then, in the final result, we will have: a factor of  $c^{d_1-1}$  if we multiply  $\tilde{\mathbf{M}}^0$ , a factor of  $c$  if we multiply  $\tilde{\mathbf{M}}^n$ , a factor of  $c^{d_2-d_1}$  if we multiply  $\tilde{\mathbf{M}}^2$ , and a factor of  $c^{N-d_2}$  if we multiply  $\tilde{\mathbf{M}}^1$ . We introduce  $[a = 1, \dots, N]$

$$\tilde{\vartheta}_a(\mathbf{q}) = e^{-\epsilon(q_a)/T} \left( e^{\mu_1/T} + \dots + e^{\mu_\kappa/T} \right), \quad (52)$$

$$f(\sigma) = \left( \frac{e^{\mu_\sigma/T}}{e^{\mu_1/T} + \dots + e^{\mu_\kappa/T}} \right), \quad \sigma = \{1, \dots, \kappa\} \quad (53)$$

and four  $N \times N$  matrices dependent on  $\mathbf{q}$  with elements

$$[\tilde{\mathbf{M}}^0(x)]_{a,b} = \tilde{\vartheta}_a^{1/2}(\mathbf{q}) \left( \int_{L_-}^x \bar{\phi}_{q_a}(z) \phi_{q_b}(z) dz \right) \tilde{\vartheta}_b^{1/2}(\mathbf{q}), \quad (54a)$$

$$[\tilde{\mathbf{M}}^1(y)]_{a,b} = \tilde{\vartheta}_a^{1/2}(\mathbf{q}) \left( \int_y^{L_+} \bar{\phi}_{q_a}(z) \phi_{q_b}(z) dz \right) \tilde{\vartheta}_b^{1/2}(\mathbf{q}), \quad (54b)$$

$$[\tilde{\mathbf{M}}^2(x, y)]_{a,b} = \tilde{\vartheta}_a^{1/2}(\mathbf{q}) \left( \int_x^y \bar{\phi}_{q_a}(z) \phi_{q_b}(z) dz \right) \tilde{\vartheta}_b^{1/2}(\mathbf{q}), \quad (54c)$$

$$[\tilde{\mathbf{M}}^n(x, y)]_{a,b} = \tilde{\vartheta}_a^{1/2}(\mathbf{q}) (\bar{\phi}_{q_a}(x) \phi_{q_b}(y)) \tilde{\vartheta}_b^{1/2}(\mathbf{q}). \quad (54d)$$

Then

$$A_\sigma(d_1, d_2 | \mathbf{q}) = \int_0^{2\pi} \frac{d\alpha}{2\pi} e^{-i(d_1-1)\alpha}$$

$$\times \int_0^{2\pi} \frac{d\beta}{2\pi} e^{-i(d_2-d_1)\beta} p_\sigma(\alpha, \beta | \mathbf{q}), \quad (55)$$

with

$$p_\sigma(\alpha, \beta | \mathbf{q}) = \det_N \left( e^{i\alpha} \tilde{\mathbf{M}}^0 - \epsilon f(\sigma) e^{i\beta} \tilde{\mathbf{M}}^2 + \tilde{\mathbf{M}}^1 + f(\sigma) \tilde{\mathbf{M}}^n \right) - \det_N \left( e^{i\alpha} \tilde{\mathbf{M}}^0 - \epsilon f(\sigma) e^{i\beta} \tilde{\mathbf{M}}^2 + \tilde{\mathbf{M}}^1 \right). \quad (56)$$

Similar to the case of the function  $h(\alpha, \beta)$  defined in (40) and analyzed in Sec. III C  $p_\sigma(\alpha, \beta | \mathbf{q})$  is a multivariate polynomial in  $e^{i\alpha}$  and  $e^{i\beta}$  with the maximum degree term given by  $e^{in_1\alpha} e^{in_2\beta}$  with  $n_1 + n_2 = N - 1$ . We have

$$p_\sigma(\alpha, \beta | \mathbf{q}) = \sum_{n_1=0}^{N-1} \sum_{n_2=0}^{N-1} a_{n_1, n_2}(\mathbf{q}) e^{i\alpha n_1} e^{i\beta n_2}, \quad (57)$$

with  $a_{n_1, n_2}(\mathbf{q}) = 0$  if  $n_1 + n_2 > N - 1$ . Because  $a_{d_1-1, d_2-d_1}(\mathbf{q}) = A_\sigma(d_1, d_2 | \mathbf{q})$  ( $d_1, d_2 = 1, \dots, N$ ) the following identity holds

$$\sum_{d_1=1}^N \sum_{d_2=d_1}^N A_\sigma(d_1, d_2 | \mathbf{q}) = \sum_{n_1=0}^{N-1} \sum_{n_2=0}^{N-1} a_{n_1, n_2}(\mathbf{q}) \equiv p_\sigma(0, 0 | \mathbf{q}), \quad (58)$$

and from (46) we obtain

$$\rho_\sigma(x, y) = \frac{1}{Z} \sum_{N=0}^{\infty} \sum_{q_1 < \dots < q_N} p_\sigma(0, 0 | \mathbf{q}). \quad (59)$$

The summation over  $N$  and  $\mathbf{q}$  can be done with the help of von Koch's determinant formula which states that for a square matrix  $A$  of dimension  $M$  (which can also be infinite) and  $z$  a complex number the following expansion holds

$$\det(\mathbf{1} + zA) = 1 + z \sum_{m=1}^M A_{m,m} + z^2 \sum_{m < n}^M \begin{vmatrix} A_{m,m} & A_{m,n} \\ A_{n,m} & A_{n,n} \end{vmatrix} + \dots \quad (60)$$

We find

$$\rho_\sigma(x, y) = \frac{1}{Z} \left[ \det \left( \mathbf{1} + \tilde{\mathbf{M}}^0 - \epsilon f(\sigma) \tilde{\mathbf{M}}^2 + \tilde{\mathbf{M}}^1 + f(\sigma) \tilde{\mathbf{M}}^n \right) - \det \left( \mathbf{1} + \tilde{\mathbf{M}}^0 - \epsilon f(\sigma) \tilde{\mathbf{M}}^2 + \tilde{\mathbf{M}}^1 \right) \right], \quad (61)$$

where now the determinants are infinite and the matrices  $\tilde{\mathbf{M}}^{0,1,2,n}$  defined in (54a), (54b), (54c), and (54d) correspond to the infinite state  $\mathbf{q} = 1, 2, \dots$ . The sum of the matrices  $\tilde{\mathbf{M}}^0$ ,  $\tilde{\mathbf{M}}^1$  and  $\tilde{\mathbf{M}}^2$  can be simplified by noticing that

$$\left[ \tilde{\mathbf{M}}^0 - \epsilon f(\sigma) \tilde{\mathbf{M}}^2 + \tilde{\mathbf{M}}^1 \right]_{a,b} = \tilde{\vartheta}_a^{1/2} \tilde{\vartheta}_b^{1/2} \left[ \left( \int_{L_-}^x -\epsilon f(\sigma) \int_x^y + \int_y^{L_+} \right) \bar{\phi}_a(z) \phi_b(z) dz \right],$$

$$\begin{aligned}
&= \tilde{\vartheta}_a^{1/2} \tilde{\vartheta}_b^{1/2} \left\{ \left[ \left( \int_{L_-}^x + \int_x^y + \int_y^{L_+} \right) - (1 + \epsilon f(\sigma)) \int_x^y \right] \bar{\phi}_a(z) \phi_b(z) dz \right\}, \\
&= \tilde{\vartheta}_a^{1/2} \tilde{\vartheta}_b^{1/2} \left[ \delta_{a,b} - (1 + \epsilon f(\sigma)) \int_x^y \bar{\phi}_a(z) \phi_b(z) dz \right]. \tag{62}
\end{aligned}$$

All that remains to be done is to divide (61) by the partition function  $Z = \prod_{q=1}^{\infty} [1 + (\sum_{\sigma=1}^{\kappa} e^{\frac{\mu_{\sigma}}{T}}) e^{-\varepsilon(q)/T}]$  which has been calculated in Appendix D. Using the result (62) and dividing the  $a$ -th row and column of the matrices appearing in (61) with  $[1 + (\sum_{\sigma=1}^{\kappa} e^{\mu_{\sigma}/T}) e^{-\varepsilon(a)/T}]^{1/2}$  we obtain the final result. The correlators in the SILL regime for an impenetrable spinor gas with  $\kappa$  components subjected to a trapping potential have the following representation

$$\rho_{\sigma}(x, y) = \det [\mathbf{1} - (1 + \epsilon f(\sigma)) \mathbf{V}_T + f(\sigma) \mathbf{R}_T] - \det [\mathbf{1} - (1 + \epsilon f(\sigma)) \mathbf{V}_T], \tag{63}$$

where  $\mathbf{V}_T$  and  $\mathbf{R}_T$  are infinite matrices with elements  $(a, b = 1, 2, \dots)$

$$[\mathbf{V}_T(x, y)]_{a,b} = (\vartheta(a)\vartheta(b))^{1/2} \int_x^y \bar{\phi}_a(z) \phi_b(z) dz, \tag{64}$$

$$[\mathbf{R}_T(x, y)]_{a,b} = (\vartheta(a)\vartheta(b))^{1/2} \bar{\phi}_a(x) \phi_b(y), \tag{65}$$

$f(\sigma)$  is defined in (53) and  $\vartheta(a)$  is a generalized Fermi function

$$\vartheta(a) = \frac{(e^{\mu_1/T} + \dots + e^{\mu_{\kappa}/T}) e^{-\varepsilon(a)/T}}{1 + (e^{\mu_1/T} + \dots + e^{\mu_{\kappa}/T}) e^{-\varepsilon(a)/T}}. \tag{66}$$

The determinant representation (63) is the generalization for arbitrary  $\kappa$  of the result derived in [83] for two-component systems.

We need to make three observations. The first observation is that (63) remains valid in nonequilibrium situations by doing a very simple modification. In the case of impenetrable particles the dynamics is restricted to the charge sector with the spin sector being frozen [83–85]. This means that out of equilibrium the spin part of the wavefunction (5) remains unchanged while the charge part is replaced by (we consider the case of a general manifold characterized by  $\mathbf{q}$ )

$$\psi_F(z_1, \dots, z_N | \mathbf{q}; t) = \frac{1}{\sqrt{N!}} \det_N [\phi_{q_j}(z_i, t)]_{i,j=1, \dots, N}, \tag{67}$$

where  $\phi_q(z, t)$  are the evolved single particle orbitals of a spinless fermionic system subjected to the same quench. Therefore, the determinant representation (63) also describe nonequilibrium situations if the relevant matrices are being replaced by  $[\mathbf{V}_T(x, y)]_{a,b} = (\vartheta(a)\vartheta(b))^{1/2} \int_x^y \bar{\phi}_a(z, t) \phi_b(z, t) dz$  and  $[\mathbf{R}_T(x, y)]_{a,b} = (\vartheta(a)\vartheta(b))^{1/2} \bar{\phi}_a(x, t) \phi_b(y, t)$ .

The second observation is that (63) can also be generalized in the case of impenetrable anyons with  $\kappa$  components [86] that satisfy the generalized commutation relations  $\Psi_{\sigma}(x) \Psi_{\sigma'}^{\dagger}(y) + e^{-i\pi\varphi \text{sgn}(x-y)} \Psi_{\sigma'}^{\dagger}(y) \Psi_{\sigma}(x) = \delta_{\sigma, \sigma'} \delta(x-y)$  and  $\Psi_{\sigma}^{\dagger}(x) \Psi_{\sigma'}^{\dagger}(y) + e^{i\pi\varphi \text{sgn}(x-y)} \Psi_{\sigma'}^{\dagger}(y) \Psi_{\sigma}^{\dagger}(x) = 0$ . Here  $\varphi \in [0, 1]$  is the statistics parameter and  $\text{sgn}(x) = |x|/x$  with  $\text{sgn}(0) = 0$ . The only modification that needs to be made is to replace  $\epsilon$  in (63) with  $-e^{-i\pi\varphi}$  for  $x \leq y$ . The fermionic (bosonic) result is reproduced for  $\varphi = 0$  ( $\varphi = 1$ ).

The third observation is that while not completely obvious the representation (63) also describes single component systems. For  $\kappa = 1$  the function  $f(\sigma) = 1$  and (63) contains as particular cases the Pezer-Buljan result [53] for single component bosons at zero temperature and the finite temperature [54] and anyonic [87] generalizations.

Let us look at certain particular cases of (63).

*No magnetic field.* In this case all the chemical potentials are equal to  $\mu$  and the Fermi function is  $\vartheta(a) = (1 + (1/\kappa)e^{(\varepsilon(a)-\mu)/T})^{-1}$ . All the correlators are equal and given by

$$\rho_{\sigma}(x, y) = \det \left[ \mathbf{1} - \left( 1 + \frac{\epsilon}{\kappa} \right) \mathbf{V}_T + \frac{1}{\kappa} \mathbf{R}_T \right] - \det \left[ \mathbf{1} - \left( 1 + \frac{\epsilon}{\kappa} \right) \mathbf{V}_T \right], \tag{68}$$

with  $\mathbf{V}_T$  and  $\mathbf{R}_T$  given by (64) and (65).

*Zero temperature case: different chemical potentials.* Without loss of generality we consider the case of  $\mu_1 > \mu_2, \dots, \mu_{\kappa}$ . At low temperatures the Fermi function becomes  $\lim_{T \rightarrow 0} \vartheta(a) \sim (1 + e^{(\varepsilon(a)-\mu_1)/T})^{-1}$  which selects only the states with  $\varepsilon(a) \leq \mu_1$ . We consider the number of states that satisfy this condition to be  $N$ . For the correlator of particles  $\sigma = 1$  we find

$$\rho_1(x, y) = \det_N \left[ \delta_{a,b} - (1 + \epsilon) \int_x^y \bar{\phi}_a(z) \phi_b(z) dz + \bar{\phi}_a(x) \phi_b(y) \right] - \det_N \left[ \delta_{a,b} - (1 + \epsilon) \int_x^y \bar{\phi}_a(z) \phi_b(z) dz \right], \tag{69}$$

which is the result derived by Pezer and Buljan [53] for single component bosons in the case  $\epsilon = 1$ . All the other correlators are zero because  $\lim_{T \rightarrow 0} f(\sigma) = 0$  for  $\sigma \neq 1$ . This shows that in the zero temperature limit a SILL system at different chemical potentials becomes fully polarized.

*Zero temperature case: equal chemical potentials.* The Fermi function selects only the  $N$  levels satisfying  $\varepsilon(a) \leq \mu$ . All the correlators are equal to

$$\rho_\sigma(x, y) = \det_N \left[ \delta_{a,b} - \left(1 + \frac{\epsilon}{\kappa}\right) \int_x^y \bar{\phi}_a(z) \phi_b(z) dz + \frac{1}{\kappa} \bar{\phi}_a(x) \phi_b(y) \right] - \det_N \left[ \delta_{a,b} - \left(1 + \frac{\epsilon}{\kappa}\right) \int_x^y \bar{\phi}_a(z) \phi_b(z) dz \right]. \quad (70)$$

### C. Dynamical fermionization of spinor gases

The determinant representations (63) can be used to study the dynamics of a spinor gas after its release from a harmonic trap. This is a common nonequilibrium scenario and in the case of the bosonic Tonks-Girardeau gas it was discovered that the asymptotic momentum distribution is equal to that of a system of free fermions in the initial harmonic trap. This phenomenon, called dynamical fermionization, was theoretically predicted in [88, 89] and experimentally confirmed in [90]. In the case of spinor gases an analytical proof of dynamical fermionization at zero temperature can be found in [84]. At finite temperature the situation is more complex. In [83] it was shown that the asymptotic momentum distribution of an impenetrable spinor gas with  $\kappa$  components at finite  $T$  and equal chemical potentials,  $\mu_\sigma = \mu$ , approaches that of a system of fermions  $n_{FF}^{\mu', T}(k) = \sum_j |\phi_j(k)|^2 / (1 + e^{-(j+1/2)-\mu'/T})$  at the same temperature but with a renormalized chemical potential

$$\mu' = \mu + T \ln \kappa. \quad (71)$$

Below, we will numerically verify this analytical prediction. This nonequilibrium scenario can be understood as a limiting case of a harmonic potential with time dependent frequency  $V(z, t) = \omega^2(t)z^2/2$  with  $\omega(t < 0) = \omega_0$  and  $\omega(t \geq 0) = 0$ . We consider an impenetrable spinor gas with  $\kappa$  components, bosonic or fermionic, which is initially in thermal equilibrium described by the grand-canonical ensemble at temperature  $T$  and equal chemical potentials  $\mu_\sigma = \mu$ ,  $\sigma = 1, \dots, \kappa$ . At  $t < 0$  the single particle orbitals are the Hermite functions  $\phi_j(z)$  of frequency  $\omega_0$ . The time-evolution of the orbitals is given by the scaling transformation ([91], Chap.VII of [92])

$$\phi_j(z, t) = \frac{1}{\sqrt{b(t)}} \phi_j\left(\frac{z}{b(t)}, 0\right) e^{i \frac{x^2}{2} \frac{\dot{b}(t)}{b(t)} - i E_j \tau(t)}, \quad (72)$$

with  $b(t)$  the solution of the second-order differential equation  $\ddot{b} + \omega^2(t)b = \omega_0^2/b^3$ , also known as the Ermakov-Pinney equation, with initial conditions  $b(0) = 1$ ,  $\dot{b}(0) = 0$  and  $\tau(t) = \int_0^t dt'/b^2(t')$ . In our case the solution of the Ermakov-Pinney equation is  $b(t) = (1 + \omega_0^2 t^2)^{1/2}$ . Inserting the scaling transformation (72) in the expressions for the wavefunctions (5) then the formula for the corre-

lator (14) becomes

$$\rho_\sigma(x, y|t) = \frac{1}{b} \rho_\sigma\left(\frac{x}{b}, \frac{y}{b} \mid 0\right) e^{-i \frac{b}{2} \frac{m(x^2 - y^2)}{2}}, \quad (73)$$

from which the momentum distribution can be computed. In Fig. 5 we present the dynamics of the momentum distribution for balanced bosonic and fermionic systems after release from the trap. We consider systems with  $\kappa = \{1, 2, 3, 4, 6\}$  and  $N = 24$  particles with  $\omega_0 = 1$  and temperature  $T = 3\omega_0$ . In both fermionic and bosonic cases after sufficient time the asymptotic momentum distribution becomes indistinguishable from the one for spinless free fermions at the same temperature and renormalized chemical potential defined in (71).

## VI. DETERMINANT REPRESENTATIONS FOR THE HOMOGENEOUS SILL CORRELATORS

The representations (63) derived in the previous section are valid for general trapping potentials or for systems with Dirichlet or Neumann boundary conditions. In the homogeneous case with periodic boundary conditions the Hamiltonian (1) is integrable and in principle one can apply the full power of Bethe ansatz techniques [4] to derive similar results. While this should be in principle doable in this section we will show that by replacing in (63) the single particle orbitals of the trapped system with the ones for the homogeneous system we obtain the previously known representations for single and two-component systems which lends credence to the argument that in fact this result is true for all values of  $\kappa$ .

The single particle orbitals for the free fermionic system with periodic boundary conditions on a ring of circumference  $L$  are  $\phi_a(z) = e^{ik_a z}/\sqrt{L}$  with  $k_a = 2\pi a/L$ ,  $a = 0, \pm 1, \dots$ . We consider the case of zero temperature with equal chemical potentials described by (70) and arbitrary statistics where  $\epsilon = -e^{i\pi\varphi}$  with  $\varphi \in [0, 1]$ . The fermionic (bosonic) case is recovered for  $\varphi = 0$  ( $\varphi = 1$ ). We have

$$\begin{aligned} \frac{1}{L} \int_x^y e^{i(k_b - k_a)z} dz &= \frac{2}{L} \frac{\sin[(k_b - k_a)(y - x)/2]}{k_b - k_a} \\ &\quad \times e^{i(k_b - k_a)y/2} e^{i(k_b - k_a)x/2}, \quad (74) \\ \frac{1}{L} e^{-ik_a x} e^{ik_b y} &= \frac{1}{L} e^{i(k_a + k_b)(y - x)/2} \end{aligned}$$

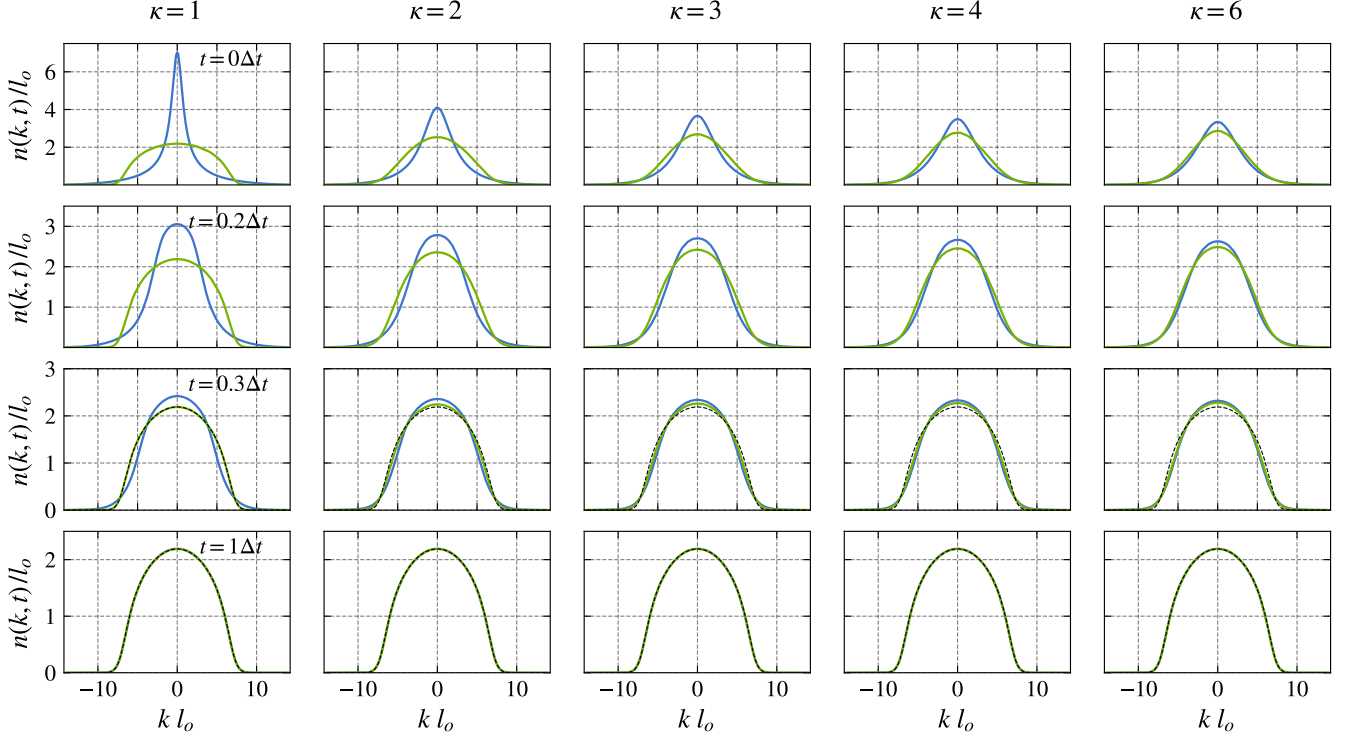


FIG. 5. Time evolution of the momentum distribution for balanced systems of bosons (blue continuous line) and fermions (green continuous line) with  $\kappa = \{1, 2, 3, 4, 6\}$  after release from a harmonic trap with  $m = \omega_0 = 1$  at finite temperature. Here  $N = 24$ ,  $T = 3\omega_0$  and the first row presents results for  $t = 0$ , the second row for  $t = 0.2\Delta t$ , the third row for  $t = 0.3\Delta t$  and the fourth row for  $t = 0.2\Delta t$  with  $\Delta t = 2\pi/\omega_0$ . In the third and fourth rows the dashed black lines represent  $n_{FF}^{\mu', T}(k)/\kappa$  with  $n_{FF}^{\mu', T}(k)$  the momentum distribution of trapped spinless fermions at the same temperature and renormalized chemical potential given by Eq. (71).

$$\times e^{i(k_b - k_a)y/2} e^{i(k_b - k_a)y/2}, \quad (75)$$

where the  $e^{i(k_b - k_a)y/2} e^{i(k_b - k_a)y/2}$  factors can be discarded because they are just a similarity transformation. Taking the thermodynamic limit  $N, L \rightarrow \infty$  such that  $D = N/L$  we find ( $x \leq y$ )

$$\rho_\sigma^h(x, y) = \det \left[ \mathbf{1} - \left( 1 - \frac{e^{i\pi\varphi}}{\kappa} \right) \hat{v} + \frac{1}{\kappa} \hat{r} \right] - \det \left[ \mathbf{1} - \left( 1 - \frac{e^{i\pi\varphi}}{\kappa} \right) \hat{v} \right], \quad (76)$$

with the result expressed in terms of Fredholm determinants of the integral operators  $\hat{v}$  and  $\hat{r}$  acting on  $[-k_F, k_F]$  ( $k_F = \pi D$ ) with kernels

$$v(k, k') = \frac{\sin[(k - k')(y - x)/2]}{\pi(k - k')}, \quad (77)$$

$$r(k, k') = \frac{e^{i(k + k')(y - x)/2}}{2\pi}. \quad (78)$$

The action of  $\hat{v}$ , and similarly of  $\hat{r}$ , on an arbitrary function  $\phi(k)$  is given by  $(\hat{v}\phi)(k) = \int_{-k_F}^{k_F} v(k, k')\phi(k') dk'$ . In the single component case,  $\kappa = 1$ , the representation (76)

is equivalent with the result for impenetrable bosons derived by Schultz [55] and Lenard [56], at  $\varphi = 0$  is equal to  $\sin[k_F(y - x)]/\pi(y - x)$ , which is the well known correlator for free fermions, and for arbitrary  $\varphi$  is the same as the result derived in [93] for impenetrable anyons. For the two-component system,  $\kappa = 2$ , (76) agrees with the result derived by Izergin and Pronko [30] for fermionic and bosonic spinor gases and the result derived in [86] for anyonic two-component gases (note that the result obtained in this section was derived under the assumption that  $x \leq y$ , for  $x > y$  one should take the complex conjugate of (76)). Therefore, we conjecture that the determinant representation (76) is also valid when  $\kappa > 2$ .

The large distance asymptotics of the static correlators can be rigorously computed using a method similar to the one employed in [25, 86] for two-component systems. The main ingredient is a very powerful result regarding the asymptotics of the generalized sine-kernel derived by Kitanine, Kozłowski, Maillet, Slavnov and Terras in [94]. Introducing two parameters

$$\xi = - \left( 1 - \frac{e^{i\pi\varphi}}{\kappa} \right), \quad \nu = - \frac{1}{2\pi i} \ln(1 + \xi) = -i \frac{\ln \kappa}{2\pi} - \frac{\varphi}{2}, \quad (79)$$

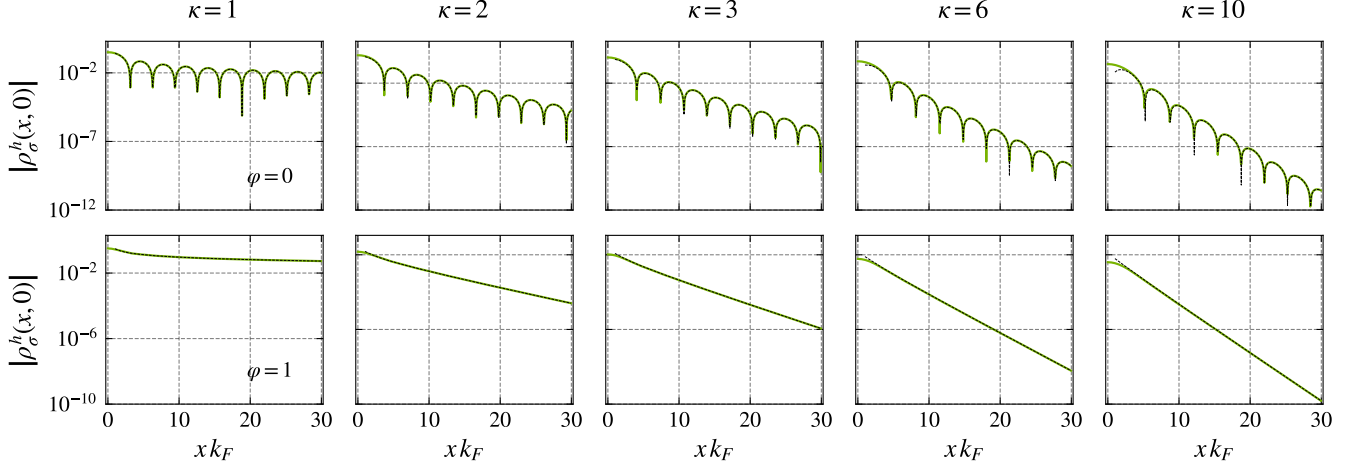


FIG. 6. Plots of the absolute value of the correlator  $|\rho_\sigma^h(x, 0)|$  (green continuous line) computed from the Fredholm determinant representation (76) and the absolute value of the asymptotics (black dashed line) given by Eq. (80) for fermionic (first row) and bosonic (second row) systems with  $\kappa = \{1, 2, 3, 6, 10\}$  and  $k_F = \pi D = 1$ .

the asymptotics are ( $x \rightarrow \infty$ )

$$\rho_\sigma^h(x, 0) = \frac{1}{\kappa} \frac{\pi e^{\mathcal{C}(\nu)}}{\xi \sin(\pi\nu)} \frac{e^{-2ik_F\nu x}}{x^{2\nu^2+1}} \times \left[ \frac{(2k_F x)^{-2\nu}}{\Gamma^2(-\nu)} e^{-ik_F x} - \frac{(2k_F x)^{2\nu}}{\Gamma^2(\nu)} e^{ik_F x} \right], \quad (80)$$

with  $\mathcal{C}(\nu) = -2\nu^2 [1 + \ln(2k_F)] + 2\nu \ln \left[ \frac{\Gamma(\nu)}{\Gamma(-\nu)} \right] - 2 \int_0^\nu \ln \left[ \frac{\Gamma(t)}{\Gamma(-t)} \right] dt$ , and  $\Gamma(t)$  is the Gamma function. For  $\kappa = 1$  the asymptotics Eq. (80) reproduce the known results for impenetrable single component bosons [95–97], impenetrable anyons [86, 98] and by taking the limit  $\varphi \rightarrow 0$  one obtains  $\sin[k_F x]/\pi x$  which is the exact result for free fermions. For two-component systems,  $\kappa = 2$ , one obtains the result for fermions derived in [22, 25, 27] for bosons derived in [49, 86] and for impenetrable anyons in [86]. For bosonic and anyonic systems described by a statistics parameter  $\varphi \sim 1$  the first term in the right hand side of (80) gives the main contribution but in the case of fermionic systems and for anyonic systems with  $\varphi \sim 0$  both terms of the expansion are important. It is important to note that our result also contains the constants in front of each term. In general these constants cannot be obtained using LL/bosonization [9, 16] or the first quantized path-integral representation for the correlators [27, 28]. The main feature of the asymptotics is the zero temperature exponential decay  $e^{-xk_F \ln \kappa/\pi}$  with an exponent proportional to the logarithm of the number of components of the system [28]. In Fig. 6 we present results for bosonic and fermionic systems with different number of components evaluated numerically [99] using the Fredholm determinant representation (76) compared with the predictions of the asymptotic formula (80). We see that we have excellent agreement, especially in the bosonic case, even though we have considered only the

first two terms of the expansion.

In the case of homogeneous spin-1/2 fermions, Matveev, Furusaki, and Glazman [100, 101] introduced an elegant method for computing the spectral function in both the Luttinger liquid and spin-incoherent regimes. Their approach involves bosonizing the charge degrees of freedom while treating the spin excitations exactly. Notably, they observed that, in addition to the expected features at  $k_F$  and  $3k_F$ , the spectral function exhibits a pronounced peak centered at  $k = 0$  (see also [102]). Whether this feature persists in systems with more than two components remains an open question. Addressing this would require generalizing the methods presented in this paper to dynamic correlators in such systems.

## VII. CONCLUSIONS

In this paper we have introduced an efficient method of computing the multidimensional integrals that appear in the expressions for the correlation functions of the strongly interacting spinor gases in 1D. While we have focused on the case of fermionic and bosonic gases it should be mentioned that our results can be applied in the case of Bose-Fermi mixtures [62, 103, 104] which present similar spin-charge factorizations of the correlators with the charge functions having identical definitions. Using this method we were able to investigate systems with a larger number of particles than considered before and we have shown that small changes in temperature have dramatic effects on the static and dynamic properties of strongly interacting spinor gases. We derived determinant representations for the correlation functions of trapped and homogeneous systems in the spin-incoherent regime and in the latter case we determined the large distance asymptotics. We expect that



our results to be generalizable in the case of the density-density correlation functions and the calculation of the full counting statistics. This is deferred to a future publication.

of Research, Innovation and Digitization is gratefully acknowledged.

## ACKNOWLEDGMENTS

Financial support from the Grant No. 30N/2023 of the National Core Program of the Romanian Ministry

## Appendix A: Fourier integral expression for the single particle densities

In this Appendix we will rewrite the expression for the single particle densities in a Fourier integral form which can be evaluated numerically in a simple fashion. The first observation that we make is that due to the fact that the product  $\bar{\psi}_F \psi_F$  appearing in Eq. (21) vanishes when two coordinates are equal and is symmetric independently in  $z_1, \dots, z_{d-1}$  and  $z_{d+1}, \dots, z_N$  we can extend the integration to  $\tilde{\Gamma}_d = L_- \leq z_1, \dots, z_d < x < z_{d+1}, \dots, z_N \leq L_+$  by multiplying the integral with  $1/(d-1)!(N-d)!$  obtaining

$$\rho_d(x) = \frac{1}{(d-1)!(N-d)!} \int_{\tilde{\Gamma}_d} \prod_{\substack{j=1 \\ j \neq d}}^N dz_j \sum_{P \in S_N} \sum_{P' \in S_N} (-1)^{P+P'} \left( \prod_{k=1}^{d-1} \bar{\phi}_{P_k}(z_k) \phi_{P'_k}(z_k) \right) \bar{\phi}_{P_d}(x) \phi_{P'_d}(x) \\ \times \left( \prod_{m=d+1}^N \bar{\phi}_{P_m}(z_m) \phi_{P'_m}(z_m) \right). \quad (\text{A1})$$

Introducing three  $N \times N$  matrices defined in (25a), (25b) and (25c) and using the fact that every permutation  $P'$  can be written as  $P' = QP$  with  $Q$  another permutation the previous relation can be rewritten as

$$\rho_d(x) = \frac{1}{(d-1)!(N-d)!} \sum_{P \in S_N} \sum_{Q \in S_N} (-1)^Q \left( \prod_{k=1}^{d-1} M_{P_k, QP_k}^0 \right) M_{P_d, QP_d}^r \left( \prod_{m=d+1}^N M_{P_m, QP_m}^1 \right). \quad (\text{A2})$$

We will show that (A2) is equivalent to

$$\rho_d(x) = \int_0^{2\pi} \frac{d\alpha}{2\pi} e^{-i(d-1)\alpha} \int_0^{2\pi} \frac{d\beta}{2\pi} e^{-i\beta} \sum_{Q \in S_N} (-1)^Q \prod_{k=1}^N (e^{i\alpha} M_{k, Qk}^0 + e^{i\beta} M_{k, Qk}^r + M_{k, Qk}^1), \quad (\text{A3})$$

expression which contains two auxiliary phase variables [30, 62, 63]. We define a set of equivalence classes on the set of permutations of  $N$  elements as follows. For a given  $d$  two permutations  $R$  and  $R'$  are equivalent, denoted by  $R \sim R'$ , if  $R = (R_1, \dots, R_{d-1}, R_d, R_{d+1}, \dots, R_N)$ ,  $R' = (R'_1, \dots, R'_{d-1}, R'_d, R'_{d+1}, \dots, R'_N)$  and  $\{R_1, \dots, R_{d-1}\} = \{R'_1, \dots, R'_{d-1}\}$  and  $\{R_{d+1}, \dots, R_N\} = \{R'_{d+1}, \dots, R'_N\}$ . This implies that  $R_d = R'_d$ . For example, if  $N = 6$  and  $d = 4$ ,  $R = (521346)$  and  $R' = (215364)$  are equivalent. We will call the representative element of a class of equivalence the permutation in which  $\{R_1, \dots, R_{d-1}\}$  and  $\{R_{d+1}, \dots, R_N\}$  are ordered. For the previous example the representative element is  $\tilde{R} = (125346)$ . For two equivalent permutations, in the sense defined above, the sum  $\sum_{Q \in S_N} (-1)^Q [\dots]$  in (A2) gives the same result. Each class of equivalence has  $(d-1)!(N-d)!$  elements which means that (A2) can be written as

$$\rho_d(x) = \sum_{\tilde{P}} \sum_{Q \in S_N} (-1)^Q \left( \prod_{k=1}^{d-1} M_{\tilde{P}_k, Q\tilde{P}_k}^0 \right) M_{\tilde{P}_d, Q\tilde{P}_d}^r \left( \prod_{m=d+1}^N M_{\tilde{P}_m, Q\tilde{P}_m}^1 \right), \quad (\text{A4})$$

where the first sum is over the representative elements which have cardinality  $N!/[(d-1)(N-d)!]$ . In (A3) each term selected by the integration over  $\alpha$  and  $\beta$  is in one-to-one correspondence with the equivalence classes of permutations (note that the integrations select  $(d-1)$  terms of  $M^0$  one of  $M^r$  and  $(N-d)$  of  $M^1$ ). For example, considering  $N = 6$ ,  $d = 4$  and  $\tilde{P} = (125346)$  the one-to-one term is  $(e^{3i\alpha} M_{1, Q_1}^0 M_{2, Q_2}^0 M_{5, Q_5}^0) (e^{i\beta} M_{3, Q_3}^r) (M_{4, Q_4}^1 M_{6, Q_6}^1)$ . This shows that (A2) and (A3) are the same. The integrand in (A3) can be written as a determinant obtaining the final expression (24).

### Appendix B: Fourier integral expression for the local exchange coefficients

The derivation of the Fourier integral expression for the local exchange coefficients (8) starts by integrating over the delta function obtaining

$$J_d^0 = N! \int_{\Gamma_d} \prod_{\substack{j=1 \\ j \neq d}}^N dz_j \left| \frac{\partial \psi_F(\mathbf{q}^0)}{\partial z_d} \right|_{z_d=z_{d+1}}^2, \quad (\text{B1})$$

with  $\Gamma_d = L_- \leq z_1 < \dots < z_{d-1} < z_{d+1} < \dots < z_N \leq L_+$ . The integrand is symmetric in  $z_1, \dots, z_{d-1}$  and  $z_{d+1}, \dots, z_N$ , so we can extend the domain of integration to  $\tilde{\Gamma}_d = L_- \leq z_1, \dots, z_{d-1} < z_{d+1}, \dots, z_N \leq L_+$  after multiplication with  $1/[(d-1)!(N-d-1)!]$ . We find

$$\begin{aligned} J_d^0 &= \frac{N!}{(d-1)!(N-d-1)!} \int_{L_-}^{L_+} dz_{d+1} \int_{L_-}^{z_{d+1}} \prod_{k=1}^{d-1} dz_k \int_{z_{d+1}}^{L_+} \prod_{m=d+2}^N dz_m \left| \frac{\partial \psi_F}{\partial z_d} \right|_{z_d=z_{d+1}}^2, \\ &= \frac{1}{(d-1)!(N-d-1)!} \int_{L_-}^{L_+} d\xi \sum_{P \in S_N} \sum_{P' \in S_N} (-1)^{P+P'} \left( \int_{L_-}^{\xi} \prod_{k=1}^{d-1} dz_k \bar{\phi}_{P_k}(z_k) \phi_{P'_k}(z_k) \right) \left( \bar{\phi}'_{P_d}(\xi) \phi'_{P'_d}(\xi) \right) \\ &\quad \times \left( \bar{\phi}_{P_{d+1}}(\xi) \phi_{P'_{d+1}}(\xi) \right) \left( \int_{\xi}^{L_+} \prod_{m=d+2}^N dz_m \bar{\phi}_{P_m}(z_m) \phi_{P'_m}(z_m) \right), \quad (\text{B2}) \end{aligned}$$

where in the second line we introduced  $z_{d+1} = \xi$ . Writing  $P' = QP$  the previous expression can be written in terms of elements of the matrices  $M^{0,1,r,d}(\xi)$  defined in (25a), (25b), (25c) and (32) as

$$\begin{aligned} J_d^0 &= \int_{L_-}^{L_+} d\xi \frac{1}{(d-1)!(N-d-1)!} \sum_{P \in S_N} \sum_{Q \in S_N} (-1)^Q \left( \prod_{k=1}^{d-1} M_{P_k, QP_k}^0(\xi) \right) M_{P_d, QP_d}^d(\xi) M_{P_{d+1}, QP_{d+1}}^r(\xi) \\ &\quad \times \left( \prod_{m=d+2}^N M_{P_m, QP_m}^1(\xi) \right). \quad (\text{B3}) \end{aligned}$$

We will denote the integrand appearing in (B3) by  $I_d(\xi)$ . Similar to the case of the single particle densities an equivalent expression of  $I_d(\xi)$  can be derived introducing three auxiliary phases with the result

$$\begin{aligned} I_d(\xi) &= \int_0^{2\pi} \frac{d\alpha}{2\pi} e^{-i(d-1)\alpha} \int_0^{2\pi} \frac{d\beta}{2\pi} e^{-i\beta} \int_0^{2\pi} \frac{d\gamma}{2\pi} e^{-i\gamma} \\ &\quad \times \sum_{Q \in S_N} (-1)^Q \prod_{k=1}^N \left( e^{i\alpha} M_{k, Qk}^0(\xi) + e^{i\beta} M_{k, Qk}^r(\xi) + e^{i\gamma} M_{k, Qk}^d(\xi) + M_{k, Qk}^1(\xi) \right), \quad (\text{B4}) \end{aligned}$$

which is exactly Eq. (31).

### Appendix C: Fourier integral expression for the one-body density matrix elements

The one-body density matrix elements are defined in (16). We consider the case  $x \leq y$  and  $d_1 \leq d_2$ . The integrand is symmetric in three set of variables  $z_1, \dots, z_{d_1-1}$ ;  $z_{d_1+1}, \dots, z_{d_2}$  and  $z_{d_2+1}, \dots, z_N$  and is zero when two of them are equal. Therefore, we can extend the domain of integration to

$$\tilde{\Gamma}_{d_1, d_2}(x, y) = L_- \leq z_1, \dots, z_{d_1-1} < x < z_{d_1+1}, \dots, z_{d_2} < y < z_{d_2+1}, \dots, z_N \leq L_+,$$

by multiplying the integral with  $1/[(d_1-1)!(d_2-d_1)!(N-d_2)!]$ . We obtain

$$\rho_{d_1, d_2}(x, y) = \frac{1}{(d_1-1)!(d_2-d_1)!(N-d_2)!} \int_{\tilde{\Gamma}_{d_1, d_2}(x, y)} \prod_{\substack{j=1 \\ j \neq d_1}}^N dz_j \sum_{P \in S_N} \sum_{P' \in S_N} (-1)^{P+P'} \left( \prod_{k=1}^{d_1-1} \bar{\phi}_{P_k}(z_k) \phi_{P'_k}(z_k) \right)$$

$$\times \left( \bar{\phi}_{P_d}(x) \phi_{P'_d}(y) \right) \left( \prod_{m=d_1+1}^{d_2} \bar{\phi}_{P_m}(z_m) \phi_{P'_m}(z_m) \right) \left( \prod_{n=d_2+1}^N \bar{\phi}_{P_n}(z_n) \phi_{P'_n}(z_n) \right). \quad (\text{C1})$$

Writing  $P' = QP$  the right hand side of (C1) becomes

$$\begin{aligned} \rho_{d_1, d_2}(x, y) &= \frac{1}{(d_1 - 1)!(d_2 - d_1)!(N - d_2)!} \sum_{P \in S_N} \sum_{Q \in S_N} (-1)^Q \left( \prod_{k=1}^{d_1-1} M_{P_k, QP_k}^0(x) \right) M_{P_{d_1}, QP_{d_1}}^n(x, y) \\ &\quad \times \left( \prod_{m=d_1+1}^{d_2} M_{P_m, QP_m}^2(x, y) \right) \left( \prod_{n=d_2+1}^N M_{P_n, QP_n}^1(y) \right), \end{aligned} \quad (\text{C2})$$

with the  $M^{0,1,2,n}$  matrices defined in (25a), (25b), (38a) and (38b). Introducing three phases this last identity can be shown to be equivalent to

$$\begin{aligned} \rho_{d_1, d_2}(x, y) &= \int_0^{2\pi} \frac{d\alpha}{2\pi} e^{-i(d_1-1)\alpha} \int_0^{2\pi} \frac{d\gamma}{2\pi} e^{-i\gamma} \int_0^{2\pi} \frac{d\beta}{2\pi} e^{-i(d_2-d_1)\beta} \\ &\quad \sum_{Q \in S_N} (-1)^Q \prod_{k=1}^N \left( e^{i\alpha} M_{k, Qk}^0 + e^{i\gamma} M_{k, Qk}^n + e^{i\beta} M_{k, Qk}^2 + M_{k, Qk}^1 \right) (x, y), \end{aligned} \quad (\text{C3})$$

which is Eq. (37) of the main text.

#### Appendix D: Partition function for the impenetrable spinor gases

The partition function of 1D impenetrable spinor gases is independent of statistics. It is instructive to consider first the particular case  $\kappa = 3$ . As we will see the generalization for arbitrary  $\kappa$  follows easily from this particular example. The partition function in the grandcanonical ensemble for  $\kappa = 3$  is

$$Z_{\kappa=3} = \sum_{N=0}^{\infty} \sum_{q_1 < \dots < q_N} \sum_{N_1=0}^N \sum_{N_2=0}^{N-N_1} \sum_{l=1}^{N!/[N_1!N_2!N_3!]} e^{-\sum_{j=1}^N \varepsilon(q_j)/T + \sum_{j=1}^3 \mu_j N_j/T}. \quad (\text{D1})$$

Because  $N!/[N_1!N_2!N_3!] = C_{N_1}^N C_{N_2}^{N-N_1}$  ( $N = N_1 + N_2 + N_3$ ) the sum over the spin eigenstates can be written as

$$\begin{aligned} \sum_{N_1=0}^N \sum_{N_2=0}^{N-N_1} C_{N_1}^N C_{N_2}^{N-N_1} e^{\sum_{j=1}^3 \mu_j N_j/T} &= \sum_{N_1=0}^N C_{N_1}^N e^{\mu_1 N_1/T} \left( e^{\mu_2/T} + e^{\mu_3/T} \right)^{N-N_1}, \\ &= \left( e^{\mu_1/T} + e^{\mu_2/T} + e^{\mu_3/T} \right)^N. \end{aligned} \quad (\text{D2})$$

Plugging this result in (D1) we obtain

$$\begin{aligned} Z_{\kappa=3} &= \sum_{N=0}^{\infty} \sum_{q_1 < \dots < q_N} \left( e^{\mu_1/T} + e^{\mu_2/T} + e^{\mu_3/T} \right)^N e^{-\sum_{j=1}^N \varepsilon(q_j)/T}, \\ &= \prod_{q=1}^{\infty} \left[ 1 + \left( e^{\mu_1/T} + e^{\mu_2/T} + e^{\mu_3/T} \right) e^{-\varepsilon(q)/T} \right]. \end{aligned} \quad (\text{D3})$$

The natural generalization for arbitrary  $\kappa$  is

$$Z = \prod_{q=1}^{\infty} \left[ 1 + \left( \sum_{\sigma=1}^{\kappa} e^{\frac{\mu_{\sigma}}{T}} \right) e^{-\varepsilon(q)/T} \right]. \quad (\text{D4})$$

- [2] X.-W. Guan, M.T. Batchelor, and C. Lee, *Fermi gases in one dimension: From Bethe ansatz to experiments*, Rev. Mod. Phys. **85**, 1633 (2013).
- [3] S.I. Mistakidis, A.G. Volosniev, R.E. Barfknecht, T. Fogarty, Th. Busch, A. Foerster, P. Schmelcher, and N.T. Zinner *Few-body Bose gases in low dimensions – a laboratory for quantum dynamics*, Phys. Rep. **1042**, 1 (2023).
- [4] V.E. Korepin, N.M. Bogoliubov, and A.G. Izergin, *Quantum Inverse Scattering Method and Correlation Functions*, (Cambridge University Press, Cambridge, UK, 1993).
- [5] F.H.L. Essler, H. Frahm, F. Göhmann, A. Klümper, and V.E. Korepin, *The One-Dimensional Hubbard Model* (Cambridge University Press, Cambridge, UK, 2005).
- [6] B. Paredes, A. Widera, V. Murg, O. Mandel, S. Fölling, I. Cirac, G. V. Shlyapnikov, T. W. Hänsch, and I. Bloch, Nature (London) **429**, 277 (2004).
- [7] T. Kinoshita, T. Wenger, and D. S. Weiss, Science **305**, 1125 (2004).
- [8] G. Pagano, M. Mancini, G. Cappellini, P. Lombardi, F. Schäfer, H. Hu, X.-J. Liu, J. Catani, C. Sias, M. Inguscio, and L. Fallani, *A One-Dimensional Liquid of Fermions with Tunable Spin*, Nature Physics **10**, 198 (2014).
- [9] T. Giamarchi, *Quantum Physics in One Dimension* (Oxford University Press, Oxford, UK, 2003).
- [10] G. Zürn, F. Serwane, T. Lompe, A. N. Wenz, M. G. Ries, J. E. Bohn, and S. Jochim, *Fermionization of Two Distinguishable Fermions*, Phys. Rev. Lett. **108**, 075303 (2012).
- [11] E. H. Lieb and W. Liniger, *Exact analysis of an interacting Bose gas, I. The general solution and the ground state*, Phys. Rev. **130**, 1605 (1963).
- [12] C. N. Yang, *Some Exact Results for the Many-Body Problem in One Dimension with Repulsive Delta-Function Interaction*, Phys. Rev. Lett. **19**, 1312 (1967).
- [13] M. Gaudin, *Un système a une dimension de fermions en interaction*, Phys. Lett. A **24**, 55 (1967).
- [14] B. Sutherland, *Further Results for the Many-Body Problem in One Dimension*, Phys. Rev. Lett. **20**, 98 (1968).
- [15] E. Lieb and D. Mattis, *Theory of Ferromagnetism and the Ordering of Electronic Energy Levels*, Phys. Rev. **125**, 164 (1962).
- [16] F.D.M. Haldane, *Effective Harmonic-Fluid Approach to Low-Energy Properties of One-Dimensional Quantum Fluids*, Phys. Rev. Lett. **47**, 1840 (1981).
- [17] E. Eisenberg and E.H. Lieb, *Polarization of Interacting Bosons with Spin*, Phys. Rev. Lett. **89**, 220403 (2002).
- [18] M.B. Zvonarev, V.V. Cheianov, and T. Giamarchi, *Spin Dynamics in a One-Dimensional Ferromagnetic Bose Gas*, Phys. Rev. Lett. **99**, 240404 (2007).
- [19] S. Akhanejee and Y. Tserkovnyak, *Spin-charge separation in a strongly correlated spin-polarized chain*, Phys. Rev. B **76**, 140408(R) (2007).
- [20] K.A. Matveev and A. Furusaki, *Spectral Functions of Strongly Interacting Isospin-1/2 Bosons in One Dimension*, Phys. Rev. Lett. **101**, 170403 (2008).
- [21] A. Kamenev and L. I. Glazman, *Dynamics of a one-dimensional spinor Bose liquid: A phenomenological approach*, Phys. Rev. A **80**, 011603(R) (2009).
- [22] A. Berkovich A and J.H. Lowenstein, *Correlation function of the one-dimensional Fermi gas in the infinite-coupling limit (repulsive case)*, Nucl. Phys. B **285**, 70 (1987).
- [23] A. Berkovich, *Temperature and magnetic field-dependent correlators of the exactly integrable (1+1)-dimensional gas of impenetrable fermions*, J. Phys. A **24** 1543 (1991).
- [24] V.V. Cheianov and M.B. Zvonarev, *Nonunitary Spin-Charge Separation in a One-Dimensional Fermion Gas*, Phys. Rev. Lett. **92**, 176401 (2004).
- [25] V.V. Cheianov and M.B. Zvonarev, *Zero temperature correlation functions for the impenetrable fermion gas*, J. Phys. A **37**, 2261 (2004).
- [26] K. A. Matveev, *Conductance of a Quantum Wire in the Wigner-Crystal Regime*, Phys. Rev. Lett. **92**, 106801 (2004).
- [27] G.A. Fiete and L. Balents, *Green's Function for Magnetically Incoherent Interacting Electrons in One Dimension*, Phys. Rev. Lett. **93**, 226401 (2004).
- [28] G.A. Fiete, *Colloquium: The spin-incoherent Luttinger liquid*, Rev. Mod. Phys. **79**, 801 (2007).
- [29] M. Ogata and H. Shiba, *Bethe-ansatz wave function, momentum distribution, and spin correlation in the one-dimensional strongly correlated Hubbard model*, Phys. Rev. B **41**, 2326 (1990).
- [30] A.G. Izergin and A.G. Pronko, *Temperature correlators in the two-component one-dimensional gas*, Nucl. Phys. B **520**, 594 (1998).
- [31] F. Deuretzbacher, K. Fredenhagen, D. Becker, K. Bongs, K. Sengstock, and D. Pfannkuche, *Exact Solution of Strongly Interacting Quasi-One-Dimensional Spinor Bose Gases* Phys. Rev. Lett. **100**, 160405 (2008).
- [32] L. Guan, S. Chen, Y. Wang, and Z. Q. Ma, *Exact Solution for Infinitely Strongly Interacting Fermi Gases in Tight Waveguides*, Phys. Rev. Lett. **102**, 160402 (2009).
- [33] F. Deuretzbacher, D. Becker, J. Bjerlin, S. M. Reimann, and L. Santos, *Quantum magnetism without lattices in strongly interacting one-dimensional spinor gases*, Phys. Rev. A **90**, 013611 (2014).
- [34] A.G. Volosniev, D.V. Fedorov, A.S. Jensen, M. Valiente, and N.T. Zinner, *Strongly interacting confined quantum systems in one dimension*, Nat. Commun. **5**, 5300 (2014).
- [35] A.G. Volosniev, D. Petrosyan, M. Valiente, D. V. Fedorov, A. S. Jensen, and N. T. Zinner, *Engineering the dynamics of effective spin-chain models for strongly interacting atomic gases*, Phys. Rev. A **91**, 023620 (2015).
- [36] J. Levinsen, P. Massignan, G.M. Bruun, and M.M. Parish, *Strong-coupling ansatz for the one-dimensional Fermi gas in a harmonic potential*, Sci. Adv. **1**, e1500197 (2015).
- [37] L. Yang, L. Guan, and H. Pu, *Strongly interacting quantum gases in one-dimensional traps*, Phys. Rev. A **91**, 043634 (2015).
- [38] L. Yang and H. Pu, *Bose-Fermi mapping and a multi-branch spin-chain model for strongly interacting quantum gases in one dimension: Dynamics and collective excitations*, Phys. Rev. A **94**, 033614 (2016).
- [39] L. Yang and X. Cui, *Effective spin-chain model for strongly interacting one-dimensional atomic gases with an arbitrary spin*, Phys. Rev. A **93**, 013617 (2016).
- [40] H. H. Jen and S.-K. Yip, *Spin-incoherent one-dimensional spin-1 Bose Luttinger liquid*, Phys. Rev. A **94**, 033601 (2016).
- [41] H. H. Jen and S.-K. Yip, *Spin-incoherent Luttinger liquid of one-dimensional spin-1 Tonks-Girardeau Bose*

- gases: *Spin-dependent properties*, Phys. Rev. A **95**, 053631 (2017).
- [42] N.J.S. Loft, L.B. Kristensen, A.E. Thomsen, and N.T. Zinner, *Comparing models for the ground state energy of a trapped onedimensional Fermi gas with a single impurity*, J. Phys. B **49**, 125305 (2016).
- [43] N.J.S. Loft, L.B. Kristensen, A.E. Thomsen, A.G. Volosniev, and N.T. Zinner, *CONAN – the cruncher of local exchange coefficients for strongly interacting confined systems in one dimension*, Comput. Phys. Commun. **209**, 171 (2016).
- [44] F. Deuretzbacher, D. Becker, and L. Santos, *Momentum distributions and numerical methods for strongly interacting one-dimensional spinor gases*, Phys. Rev. A **94**, 023606 (2016).
- [45] R.E. Barfknecht, A. Foerster, and N.T. Zinner, *Dynamics of spin and density fluctuations in strongly interacting few-body systems*, Sci Rep **9**, 15994 (2019).
- [46] P. Capuzzi, L. Tessieri, Z. Akdeniz, A. Minguzzi, and P. Vignolo, *Spin-charge separation in the quantum boomerang effect*, Phys. Rev. A **109**, 063315 (2024).
- [47] L. Yang and H. Pu, *One-body density matrix and momentum distribution of strongly interacting one-dimensional spinor quantum gases*, Phys. Rev. A **95**, 051602(R) (2017).
- [48] H. H. Jen and S.-K. Yip, *Spin-incoherent Luttinger liquid of one-dimensional  $SU(\kappa)$  fermions*, Phys. Rev. A **98**, 013623 (2018).
- [49] V.V. Cheianov, H. Smith, and M.B. Zvonarev, *Low-temperature crossover in the momentum distribution of cold atomic gases in one dimension*, Phys. Rev. A **71**, 033610 (2005).
- [50] O.I. Păţu, A. Klümper and A. Foerster, *Universality and quantum criticality of the one-dimensional spinor Bose gas*, Phys. Rev. Lett. **120**, 243402 (2018).
- [51] P. Capuzzi and P. Vignolo, *Finite-temperature contact for a  $SU(2)$  Fermi gas trapped in a one-dimensional harmonic confinement*, Phys. Rev. A **101**, 013633 (2020).
- [52] G. Pecci, P. Vignolo, and A. Minguzzi, *Universal spin-mixing oscillations in a strongly interacting one-dimensional Fermi gas*, Phys. Rev. A **105**, L051303 (2022).
- [53] R. Pezer and H. Buljan, *Momentum Distribution Dynamics of a Tonks-Girardeau Gas: Bragg Reflections of a Quantum Many-Body Wave Packet*, Phys. Rev. Lett. **98**, 240403 (2007).
- [54] Y. Y. Atas, D. M. Gangardt, I. Bouchoule, and K. V. Kheruntsyan, *Exact nonequilibrium dynamics of finite-temperature Tonks-Girardeau gases*, Phys. Rev. A **95**, 043622 (2017).
- [55] T.D. Schultz, *Note on the one-dimensional gas of impenetrable point-particle bosons*, J. Math. Phys. **4**, 666 (1963).
- [56] A. Lenard, *One-dimensional impenetrable bosons in thermal equilibrium*, J. Math. Phys. **7**, 1268 (1966).
- [57] L. Yang, S.S. Alam, and H. Pu, *Generalized Bose-Fermi mapping and strong coupling ansatz wavefunction for one dimensional strongly interacting spinor quantum gases*, J. Phys. A **55**, 464005 (2022).
- [58] A. Minguzzi and P. Vignolo, *Strongly interacting trapped one-dimensional quantum gases: Exact solution*, AVS Quantum Sci. **4**, 027102 (2022).
- [59] A. Dehkharghani, A. Volosniev, J. Lindgren, J. Rotureau, C. Forssén, D. Fedorov, A. Jensen, and N.Zinner, *Quantum magnetism in strongly interacting one-dimensional spinor Bose systems*, Sci. Rep. **5**, 10675 (2015).
- [60] J. Decamp, J. Jünemann, M. Albert, M. Rizzi, A. Minguzzi, and P. Vignolo, *High-momentum tails as magnetic-structure probes for strongly correlated  $SU(\kappa)$  fermionic mixtures in one-dimensional traps*, Phys. Rev. A **94**, 053614 (2016).
- [61] A. Osterloh, J. Polo, W.J. Chetcuti, and L. Amico, *Exact one-particle density matrix for  $SU(N)$  fermionic matter-waves in the strong repulsive limit*, SciPost Phys. **15**, 006 (2023).
- [62] A. Imambekov and E. Demler, *Applications of exact solution for strongly interacting one dimensional bose-fermi mixture: low-temperature correlation functions, density profiles and collective modes*, Ann. Phys. (NY) **321**, 2390 (2006).
- [63] O.I. Păţu, *Dynamical fermionization in a one-dimensional Bose-Fermi mixture*, Phys. Rev. A **105**, 063309 (2022).
- [64] M. Marcus, *Determinants of sums*, College Math. J. **21**, 130 (1990).
- [65] D.H. Bailey and P.N. Swarztrauber, *The Fractional Fourier Transform and Applications* SIAM Rev. **33**, 389 (1991).
- [66] G.W. Inverarity, *Fast Computation of Multidimensional Fourier Integrals*, SIAM J. Sci. Comput. **24**, 645 (2002).
- [67] J.C. Piquette, *A method for symbolic evaluation of indefinite integrals containing special functions or their products*, J. Symbol. Comput. **11**, 231 (1991).
- [68] W. H. Press, B. P. Flannery, S. A. Teukolsky, and W. T. Vetterling, *Numerical Recipes in C: The Art of Scientific Computing* (Cambridge University Press, Cambridge, England, 1992).
- [69] W.J. Chetcuti, A. Osterloh, L. Amico, and J. Polo, *Interference dynamics of matter-waves of  $SU(N)$  fermions*, SciPost Phys. **15**, 181 (2023).
- [70] S. Tan, *Energetics of a strongly correlated Fermi gas*, Ann. Phys. **323**, 2952 (2008).
- [71] S. Tan, *Large momentum part of a strongly correlated Fermi gas*, Ann. Phys. **323**, 2971 (2008).
- [72] S. Tan, *Generalized virial theorem and pressure relation for a strongly correlated Fermi gas*, Ann. Phys. **323**, 2987 (2008).
- [73] M. Olshanii and V. Dunjko, *Short-Distance Correlation Properties of the Lieb-Liniger System and Momentum Distributions of Trapped One-Dimensional Atomic Gases*, Phys. Rev. Lett. **91**, 090401 (2003).
- [74] M. Valiente, N.T. Zinner, and K. Mølmer, *Universal properties of Fermi gases in arbitrary dimensions*, Phys. Rev. A **86**, 043616 (2012).
- [75] M. Barth and W. Zwerger, *Tan relations in one dimension*, Ann. Phys. **326**, 2544 (2011).
- [76] O.I. Păţu and A. Klümper, *Universal Tan relations for quantum gases in one dimension*, Phys. Rev. A **96**, 063612 (2017).
- [77] D. Cavazos-Cavazos, R. Senaratne, A. Kifle, and R.G. Hulet, *Thermal disruption of a Luttinger liquid*, Nature Communications **14**, 3154 (2023).
- [78] G. Aupetit-Diallo, G. Pecci, C. Pignol, F. Hébert, A. Minguzzi, M. Albert, and P. Vignolo, *Exact solution for  $SU(2)$ -symmetry-breaking bosonic mixtures at strong interactions*, Phys. Rev. A **106**, 033312 (2022).
- [79] S. Musolino, M. Albert, A. Minguzzi, and P. Vig-



- nolo, *Symmetry oscillations in strongly interacting one-dimensional mixtures*, [arXiv:2407.00194](#).
- [80] V.B. Bulchandani, S. Gopalakrishnan, and E. Ilievski, *Superdiffusion in spin chains*, J. Stat. Mech. 084001, (2021).
  - [81] C. P. Moca, M. A. Werner, A. Valli, T. Prosen, and G. Zaránd, *Kardar-Parisi-Zhang scaling in the Hubbard model*, Phys. Rev. B **108**, 235139 (2023).
  - [82] M. Kardar, G. Parisi, and Y.-C. Zhang, *Dynamic scaling of growing interfaces*, Phys. Rev. Lett. **56**, 889 (1986).
  - [83] O.I. Pătu, *Nonequilibrium dynamics in one-dimensional strongly interacting two-component gases*, Phys. Rev. A **108**, 053304 (2023).
  - [84] S.S. Alam, T. Skaras, L. Yang, and H. Pu, *Dynamical fermionization in one-dimensional spinor quantum gases*, Phys. Rev. Lett. **127**, 023002 (2021).
  - [85] O.I. Pătu, *Dynamical Fermionization in One-Dimensional Spinor Gases at Finite Temperature*, Phys. Rev. Lett. **130**, 163201 (2023).
  - [86] O.I. Pătu, *Correlation functions of one-dimensional strongly interacting two-component gases*, Phys. Rev. A **100**, 063635 (2019).
  - [87] O.I. Pătu, *Nonequilibrium dynamics of the anyonic Tonks-Girardeau gas at finite temperature*, Phys. Rev. A **102**, 043303 (2020).
  - [88] M. Rigol and A. Muramatsu, *Fermionization in an expanding 1D gas of hard-core Bosons*, Phys. Rev. Lett. **94**, 240403 (2005).
  - [89] A. Minguzzi and D.M. Gangardt, *Exact coherent states of a harmonically confined Tonks-Girardeau gas*, Phys. Rev. Lett. **94**, 240404 (2005).
  - [90] J.M. Wilson, N. Malvania, Y. Le, Y. Zhang, M. Rigol, and D. S. Weiss, *Observation of dynamical fermionization*, Science **367**, 1461 (2020).
  - [91] V.S. Popov and A.M. Perelomov, *Parametric excitation of a quantum oscillator II*, Zh. Eksp. Teor. Fiz. **57**, 1684 (1970). [JETP **30**, 910 (1970)].
  - [92] A.M. Perelomov and Y.B. Zel'dovich, *Quantum Mechanics: Selected Topics* (World Scientific, Singapore, 1998).
  - [93] O.I. Pătu, V.E. Korepin, and D.V. Averin, *One-dimensional impenetrable anyons in thermal equilibrium: II. Determinant representation for the dynamic correlation functions*, J. Phys. A **41**, 255205 (2008).
  - [94] N. Kitanine, K. K. Kozłowski, J. M. Maillet, N. A. Slavnov, and V. Terras, *Riemann-Hilbert approach to a generalized sine kernel and applications*, Commun. Math. Phys. **291**, 691 (2009).
  - [95] H.G. Vaidya and C.A. Tracy, *One-Particle Reduced Density Matrix of Impenetrable Bosons in One Dimension at Zero Temperature*, Phys. Rev. Lett. **42**, 3 (1979).
  - [96] M. Jimbo, T. Miwa, Y. Mori and M. Sato, *Density matrix of an impenetrable Bose gas and the fifth Painlevé transcendent*, Physica D (Amsterdam) **1**, 80 (1980).
  - [97] D.M. Gangardt, *Universal correlations of trapped one-dimensional impenetrable bosons*, J. Phys. A **37**, 9335 (2004).
  - [98] P. Calabrese and M. Mintchev, *Correlation functions of one-dimensional anyonic fluids*, Phys. Rev. B **75**, 233104 (2007).
  - [99] F. Bornemann, *On the numerical evaluation of Fredholm determinants*, Math. Comp. **79**, 871 (2010).
  - [100] K.A. Matveev, A. Furusaki, and L. I. Glazman, *Asymmetric Zero-Bias Anomaly for Strongly Interacting Electrons in One Dimension*, Phys. Rev. Lett. **98**, 096403 (2007).
  - [101] K.A. Matveev, A. Furusaki, and L. I. Glazman, *Bosonization of strongly interacting one-dimensional electrons*, Phys. Rev. B **76**, 155440 (2007).
  - [102] G.A. Fiete, J. Qian, Y. Tserkovnyak, and B.I. Halperin, *Theory of momentum resolved tunneling into a short quantum wire*, Phys. Rev. B **72**, 045315 (2005).
  - [103] J. Decamp, J. Jünemann, M. Albert, M. Rizzi, A. Minguzzi, and P. Vignolo, *Strongly correlated one-dimensional Bose-Fermi quantum mixtures: symmetry and correlations*, New J. Phys. **19**, 125001 (2017).
  - [104] F. Deuretzbacher, D. Becker, J. Bjerlin, S.M. Reimann, and L. Santos, *Spin-chain model for strongly interacting one-dimensional Bose-Fermi mixtures*, Phys. Rev. A **95**, 043630 (2017).